

ADAPTIVE FINITE ELEMENT APPROXIMATIONS FOR ELLIPTIC PROBLEMS USING REGULARIZED FORCING DATA*

LUCA HELTAI[†] AND WENYU LEI[†]

Abstract. We propose an adaptive finite element algorithm to approximate solutions of elliptic problems whose forcing data is locally defined and is approximated by regularization (or mollification). We show that the energy error decay is quasi-optimal in two dimensional space and sub-optimal in three dimensional space. Numerical simulations are provided to confirm our findings.

Key words. Finite elements, interface problems, immersed boundary method, Dirac delta approximations, a posteriori error estimates, adaptivity

AMS subject classifications. 65N15, 65N30, 65N50,

1. Introduction. Let us consider the numerical approximation of the following elliptic problem with rough data: given a bounded domain $\Omega \subset \mathbb{R}^d$ with $d = 2$ or 3 , we seek a distribution u satisfying

$$(1.1) \quad \begin{aligned} -\nabla \cdot (A(x)\nabla u) + c(x)u &= F, & \text{in } \Omega, \\ u &= 0, & \text{on } \partial\Omega. \end{aligned}$$

Here $A(x)$ is a $d \times d$ symmetric positive definite matrix with all entries in $C^1(\bar{\Omega})$. We further assume that there exist positive constants a_0 and a_1 satisfying

$$(1.2) \quad a_0|\nu|^2 \leq \nu^\top A(x)\nu \leq a_1|\nu|^2, \quad \text{for all } \nu \in \mathbb{R}^d \text{ and } x \in \bar{\Omega}.$$

The lower order coefficient $c(x)$ is set to be non-negative and Lipschitz in $\bar{\Omega}$. We consider rough forcing data F that can be written as

$$F(x) := \int_B \delta(x-y)f(y) dy, \quad \text{with } B \subset \Omega,$$

where δ denotes the d -dimensional Dirac distribution and $B \subset \mathbb{R}^d$ is an immersed domain. If the co-dimension of B is zero, $F(x) = \chi_B(x)f(x)$ with χ_B denoting the indicator function of B . If the co-dimension of B is one, F can be written as a distribution. That is

$$(1.3) \quad \langle F, \phi \rangle := \int_B f(y)\phi(y) dy, \quad \text{for all } \phi \in C_c^\infty(\bar{\Omega}).$$

In the rest of the paper, our discussion on the numerical approximation of (1.1) will be restricted to the co-dimension one case.

The above elliptic problem is a prototype of governing differential equations for interface problems, phase transitions and fluid-structure interactions problems using the immersed boundary method [35, 9, 36, 40]. Many works exist that concentrate on

*Draft date: October 29, 2021

Funding: This work was partially supported by the National Research Projects (PRIN 2017) “Numerical Analysis for Full and Reduced Order Methods for the efficient and accurate solution of complex systems governed by Partial Differential Equations”, funded by the Italian Ministry of Education, University, and Research.

[†]Mathematics Area, SISSA – International School for Advanced Studies, via Bonomea 265, 34136, Trieste, Italy (luca.heltai@sissa.it, wenyu.lei@sissa.it).

the study of (adaptive) finite element methods with point Dirac sources [5, 29, 1]. The relevant literature for more complex distributions of singularities is more limited [31, 30]. The motivation for such methods lies on the possibly complex geometry of the immersed domain, such as thin vascular structures in tissues [23, 24, 13] or fibers in isotropic materials [2], for which it is difficult to obtain a bulk mesh of Ω matching the embedded domain.

On the the other hand, when considering a non-matching bulk mesh to approximate problem (1.1), it is necessary to evaluate F on the quadrature points of Ω or to compute (1.3) when ϕ is a test function in a finite dimensional space. The implementation of the former strategy was introduced by Peskin in the early seventies (see [35] for a review) in the context of finite differences, and later adopted to finite volume and finite element approaches [33]. The latter approximation strategy, usually referred to as the “variational formulation”, was introduced in [8] and later works, for example [25].

Since the data function is not smooth, classical numerical quadrature schemes defined on cells in the non-matching mesh could lose the accuracy. To resolve this, one could develop quadrature schemes depending on the immersed domain. Here we consider an alternative approach by approximating F with its regularization (or mollification) [28, 41]. That is, we replace δ with a family of Dirac delta approximations δ^r , where r denotes the regularization parameter so that the regularized data, denoted by F^r , satisfies certain smoothness property. The error between the exact solution u and its regularized counterpart u^r is analyzed in [26] in both the H^1 and L^2 sense. The finite element approximation of (1.1) using quasi-uniform subdivisions is also discussed in [26].

In this paper, we consider the finite element approximation of (1.1) with the regularized data F^r under adaptive subdivisions. Adaptive finite element methods (AFEMs) have been widely used for decades; see [34] for a survey of AFEMs for elliptic problems. In terms of the singular data F , we refer to [38, 37] for piecewise constant approximation of F and [15] using surrogate data indicators.

The approximation error based on regularized data consists of two parts: the regularization error for u and the finite element approximation error for u^r . The analysis of adaptive algorithms applied to the regularized problem is complicated by the fact that optimal choices of the regularization parameter r depend on the local mesh size h (see [26]), and that the error estimates depend both on the local mesh size and on the regularization parameter r .

We present our algorithm in Section 3. We control each error in a separate routine: the routine `INTERFACE` controls the first error using the perturbation theory built in [26] (see also Proposition 2.7) and returns the optimal regularization parameter r to use in the routine `SOLVE`, which controls the error of the regularized problem using classic AFEM results based on [15].

Given a target tolerance, the `INTERFACE` routine refines *a priori* the cells around the immersed domain so that the regularization error can be properly controlled. This procedure ensures that the regularization parameter r is suitable for the local mesh size around the immersed domain. Given the regularization parameter r , the `SOLVE` routine will then approximate the regularized problem using AFEM based on [15] so that the finite element error can also be reduced below the desired tolerance. Our complete algorithm is based on the iteration of the two routines above with a decaying target tolerance.

The performance of our adaptive algorithm is studied adapting the theories from [15, 10] to our regularized problem. The major point to take into account is that all

the estimates one obtains are generally dependent on the regularization parameter r , which in turn is generally chosen according to the local mesh size h . More precisely speaking, the following two issues must be analyzed carefully:

- For any $r > 0$, the regularized solutions u^r are in some approximation class \mathcal{A}^s for some $s \in (0, \frac{1}{d}]$ (see Section 4.2 for the definition) and the corresponding quasi-semi-norms are uniformly bounded.
- The regularized data F^r is in $L^2(\Omega)$, and we can guarantee that there exists an adaptive method to approximate F^r with a quasi-optimal rate (cf. [15, Theorem 7.4]). However, the bounds on the L^2 norm of the regularized data depend on (negative) powers of the regularization parameter r , i.e., of the local mesh size h , inducing a deterioration of the convergence rates.

To remedy the second issue, in Lemma 4.7, we provide a finer estimate by using the fact that F^r is supported in the neighborhood of the immersed domain. To resolve the first issue, we follow the arguments from [10]. Thanks to the *a priori* refinements from the INTERFACE part of the algorithm, Lemma 3.2 of [10] allows us to measure the complexity of SOLVE stage independently of r . In Theorem 4.16 and Remark 4.17, we show that our algorithm is quasi-optimal in 2d with respect to the energy norm and sub-optimal in 3d.

The rest of this article is organized as follows. In Section 2 we provide some essential notations to define our model problem in the variational sense, and we introduce the data regularization (or data mollification) as well as a regularized version of the model problem. In Section 3 we review the AFEM for elliptic problems with $L^2(\Omega)$ forcing data. Following this approach, we then propose our adaptive algorithm for the model problem. In Section 5 we provide some numerical experiments to illustrate the performance of our proposed algorithm. The analysis of the adaptive algorithm is presented in Section 4. We conclude with some remarks in Section 6.

Notations and Sobolev spaces. Let $\Omega \subset \mathbb{R}^d$ be a bounded Lipschitz domain. We write $A \lesssim B$ if $A \leq cB$ for some constant c independent of A , B and other discretization parameters. We say $A \sim B$ if $A \lesssim B$ and $B \lesssim A$.

Given a Hilbert space X , we denote with $(\cdot, \cdot)_X$ its inner product, and with X' its dual space with the induced norm

$$\|F\|_{X'} = \sup_{\|v\|_X=1} \langle F, v \rangle_{X', X},$$

where $\langle \cdot, \cdot \rangle_{X', X}$ denotes the duality pairing.

We indicate with $L^2(\Omega)$, $H^1(\Omega)$ and $H^2(\Omega)$ the usual Sobolev spaces and use $(\cdot, \cdot)_\Omega$ to indicate the $L^2(\Omega)$ -inner product. For $s \in (0, 1)$, we denote the fractional Sobolev spaces $H^s(\Omega)$ using the Sobolev–Slobodeckij norm

$$\|v\|_{H^s(\Omega)} := \left(\|v\|_{L^2(\Omega)}^2 + \int_{\Omega} \int_{\Omega} \frac{(v(x) - v(y))^2}{|x - y|^{d+2s}} dx dy \right)^{1/2}.$$

For $s \in (1, 2)$,

$$\|v\|_{H^s(\Omega)} = \left(\|v\|_{L^2(\Omega)}^2 + \|\nabla v\|_{H^{s-1}(\Omega)}^2 \right)^{1/2}.$$

For $s \in (\frac{1}{2}, 1]$, we set $H_0^s(\Omega)$ to be the collection of functions in $H^1(\Omega)$ vanishing on $\partial\Omega$. It is well known that $H_0^s(\Omega)$ is the closure of $C_c^\infty(\bar{\Omega})$ (the space of infinitely differentiable functions with compact support in $\bar{\Omega}$) with respect to the norm of $H^s(\Omega)$ (cf. [22]). Also, $H_0^s(\Omega)$ is an interpolation space between $L^2(\Omega)$ and $H_0^1(\Omega)$ using the real method. Finally for $s \in (\frac{1}{2}, 1]$, we set $H^{-s}(\Omega) = H_0^s(\Omega)'$.

2. Model problem and its regularization. In this section, we will introduce the variational formulation of our model problem as well as a formulation when the forcing data F is approximated by regularization.

2.1. The forcing data. Let $\omega \subset \Omega$ be a bounded domain and let $\gamma := \partial\omega$ be its boundary, which we take to be of class C^2 . In what follows, we only consider the case when γ is away from $\partial\Omega$, i.e., there exists a positive constant c_γ such that

$$(2.1) \quad \text{dist}(\gamma, \partial\Omega) > c_\gamma.$$

We assume that the data function $f \in L^\infty(\gamma)$, and we further assume that there exists a finite collection of possibly overlapping non empty open sets $\{\gamma_j \subset \gamma\}_{j=1}^{M_\gamma}$ such that f does not change sign on each γ_j , and that

$$(2.2) \quad \sum_{j=1}^{M_\gamma} |\gamma_j| \lesssim |\gamma|.$$

We then consider a forcing data that can be formally written as

$$(2.3) \quad F = \mathcal{M}f := \int_\gamma \delta(x-y)f(y) d\sigma_y.$$

The variational definition of F (see, i.e., [26]) implies that that $F \in H^{-s}(\Omega) \subset H^{-1}(\Omega)$ with any fixed $s \in (\frac{1}{2}, 1]$. In fact, for any $v \in H_0^1(\Omega)$, there holds

$$(2.4) \quad \begin{aligned} \langle F, v \rangle_{H^{-1}(\Omega), H_0^1(\Omega)} &= \int_\gamma f v d\sigma \\ &\leq \|f\|_{L^2(\gamma)} \|v\|_{L^2(\gamma)} \\ &\lesssim \|f\|_{L^2(\gamma)} \|v\|_{H^s(\omega)} \lesssim \|f\|_{L^2(\gamma)} \|v\|_{H^s(\Omega)}, \end{aligned}$$

where for the first inequality above we applied Schwartz inequality and for the second inequality we used the trace inequality.

2.2. Weak formulation. The variational formulation of (1.1) reads: given a function $f \in L^2(\gamma)$, we seek $u \in H_0^1(\Omega)$ such that

$$(2.5) \quad A(u, v) = \langle F, v \rangle_{H^{-1}(\Omega), H_0^1(\Omega)}, \quad \text{for all } v \in H_0^1(\Omega),$$

where

$$A(v, w) = \int_\Omega \nabla v^\top A(x) \nabla w + c(x)vw dx, \quad \text{for all } v, w \in H_0^1(\Omega).$$

Assumption (1.2) and the non-negativity of $c(x)$ guarantee that the bilinear form $A(\cdot, \cdot)$ is bounded and coercive, i.e., there exist positive constants m, M so that for $v, w \in H_0^1(\Omega)$,

$$(2.6) \quad A(v, w) \leq M \|v\|_{H^1(\Omega)} \|w\|_{H^1(\Omega)} \text{ and } A(v, v) \geq m \|v\|_{H^1(\Omega)}^2,$$

and (2.5) admits a unique solution by Lax-Milgram Lemma. Bound (2.6) also implies that $\|v\| := \sqrt{A(v, v)} \sim \|v\|_{H^1(\Omega)}$. In what follows, we use the energy norm $\|\cdot\|$ instead of $\|\cdot\|_{H^1(\Omega)}$ in our adaptive algorithm as well as in the performance analysis.

2.3. Regularization. The regularization of F is based on the approximation of the Dirac delta distribution. To this end, we first define a class of functions ψ satisfying the following assumptions:

Assumption 2.1. Given $k \in \mathbb{N}$, let $\psi(x)$ in $L^\infty(\mathbb{R}^d)$ such that

1. **Nonnegativity:** $\psi(x) \geq 0$;
2. **Compact support:** $\psi(x)$ is compactly supported, with support $\text{supp}(\psi)$ contained in $B_{r_0}(0)$ (the ball centered in zero with radius r_0) for some $r_0 > 0$;
3. **Moments condition:** Given $k \in \mathbb{N}$, we say ψ satisfies the k -th order moment condition if

$$(2.7) \quad \int_{\mathbb{R}^d} y_i^\alpha \psi(x-y) dy = x_i^\alpha \quad i = 1 \dots d, \quad 0 \leq \alpha \leq k, \quad \text{for all } x \in \mathbb{R}^d;$$

Using the above ψ , for $r > 0$, we define the Dirac approximation δ^r by

$$(2.8) \quad \delta^r(x) := \frac{1}{r^d} \psi\left(\frac{x}{r}\right).$$

Thus,

$$\lim_{r \rightarrow 0} \delta^r(x) = \lim_{r \rightarrow 0} \frac{1}{r^d} \psi\left(\frac{x}{r}\right) = \delta(x),$$

where the limit should be understood in the space of Schwartz distributions.

Remark 2.2 (nonnegativity of ψ). We shall use the non-negativity of ψ to analyze the performance of our adaptive algorithm. However, this is not required in the error analysis for finite element discretization of (1.1) using quasi-uniform subdivisions of Ω ; see [26] for more details.

Remark 2.3 (generating Dirac delta approximations). There are two common class of $\psi(x)$ in practice. The first class can be formed by choosing a one dimensional function $\psi_\rho \in L^\infty(\mathbb{R})$ so that ψ_ρ is supported in $[0, 1]$. Then we define the function ψ in \mathbb{R}^d as the radially symmetric extension of ψ_ρ with respect to the origin, i.e.,

$$(2.9) \quad \psi(x) := I_d \psi_\rho(|x|),$$

where I_d is a scaling factor, chosen so that $\psi(x)$ integrates to one (i.e., it satisfies the zero-th order moment condition). With this choice, ψ is also symmetric and it satisfies Assumption 2.1 with $k \geq 1$. The second class is usually referred to as tensor product construction (cf. [28]). We start from a $L^\infty(\mathbb{R})$ function ψ_{1d} that satisfies Assumption 2.1 for some k in \mathbb{R} . Then we set $\psi(x)$ in dimension d by

$$(2.10) \quad \psi(x) := \prod_{i=1}^d \psi_{1d}(x_i), \quad \text{for } x = (x_1, \dots, x_d) \in \mathbb{R}^d.$$

This construction of $\psi(x)$ satisfies Assumption 2.1 with the same order k of ψ_{1d} . In particular $k = 0$ if ψ_{1d} is not symmetric, and k is equal to at least one if ψ_{1d} is symmetric; we refer to [28, 41] for more discussions on other possible choices of Dirac approximation classes $\psi(x)$.

DEFINITION 2.4 (Regularization). *For a function $v \in L^1(\Omega)$ we define its regularization $v^r(x)$ in the domain Ω through the mollifier ψ by*

$$(2.11) \quad v^r(x) := \int_{\Omega} \delta^r(x-y)v(y) dy, \quad \text{for all } x \in \Omega,$$

where δ^r is given by (2.8) and where ψ satisfies Assumption 2.1 for some $k \geq 0$.

For functionals F in negative Sobolev spaces, say $F \in H^{-s}(\Omega)$, with $s \in (\frac{1}{2}, 1]$, we define their regularization F^r by the action of F on v^r with $v \in H_0^s(\Omega)$, i.e.,

$$(2.12) \quad \langle F^r, v \rangle_{H^{-s}(\Omega), H_0^s(\Omega)} := \langle F, v^r \rangle_{H^{-s}(\Omega), H_0^s(\Omega)}.$$

We note that the definition of F^r is well defined with F given by (2.3). In fact, by [26, Corollary 1], there holds

$$\|v - v^r\|_{H^s(\omega)} \lesssim \|v\|_{H^s(\Omega)}.$$

Therefore, according to the argument in (2.4), we have

$$\langle F^r, v \rangle_{H^{-s}(\Omega), H_0^s(\Omega)} \lesssim \|f\|_{L^2(\gamma)} \|v^r\|_{H^s(\omega)} \lesssim \|f\|_{L^2(\gamma)} \|v\|_{H^s(\Omega)}.$$

Remark 2.5. For F defined by (2.3), applying Fubini's Theorem to the right hand side of (2.12) yields

$$F^r(x) = \int_{\gamma} f(y) \delta^r(y-x) dy \in L^2(\Omega).$$

If ψ is chosen to be symmetric, the definition of F^r can be interpreted by replacing δ in (2.3) with the Dirac approximation δ^r .

Remark 2.6 (Error estimate of the regularization). Lemma 10 of [26] implies that the following regularization error estimates holds when $r < 1$,

$$(2.13) \quad \|F - F^r\|_{H^{-1}(\Omega)} \leq C_{\text{reg}} r^{1/2} \|f\|_{L^2(\gamma)}$$

where the constant C_{reg} depends on ψ in Assumption 2.1 and ω .

2.4. Regularized problem. A regularized version of problem (2.5) reads: find $u^r \in H_0^1(\Omega)$ satisfying

$$(2.14) \quad A(u^r, v) = \langle F^r, v \rangle_{H^{-1}(\Omega), H_0^1(\Omega)}, \quad \text{for all } v \in H_0^1(\Omega).$$

Notice that u^r exists and is unique. Moreover, (2.6) and Remark 2.6 imply that

$$\begin{aligned} \| \|u - u^r\| \|^2 &= A(u - u^r, u - u^r) \\ &= \langle F - F^r, u - u^r \rangle_{H^{-1}(\Omega), H_0^1(\Omega)} \\ &\leq m^{-1/2} \|F - F^r\|_{H^{-1}(\Omega)} \| \|u - u^r\| \| \\ &\leq m^{-1/2} C_{\text{reg}} r^{1/2} \|f\|_{L^2(\gamma)} \| \|u - u^r\| \|. \end{aligned}$$

Hence we obtain the following perturbation estimate.

PROPOSITION 2.7 (see also Theorem 14 of [26]). *When Assumption 2.1 holds, let u and u^r be the solution to (2.5) and (2.14), respectively. Then there holds*

$$(2.15) \quad \| \|u - u^r\| \| \leq m^{-1/2} C_{\text{reg}} r^{1/2} \|f\|_{L^2(\gamma)}.$$

3. Numerical algorithm. We approximate the solution to the weak formulation (2.5) by solving the regularized problem (2.14) using AFEMs along with regularization parameter r . As the number of degrees of freedom increase, r will tend to zero with a rate linked to the target tolerance. Recalling from Remark 2.5, the regularized data F^r is an $L^2(\Omega)$ function so that we can use classical residual error estimators for adaptivity. In this section, we first review AFEMs for elliptic problems with $L^2(\Omega)$ forcing data based on [15, 38, 34]. Then we introduce our adaptive algorithm for (2.5).

3.1. Finite element approximation. We additionally assume that Ω is a polytope. Given a data function $g \in L^2(\Omega)$, we consider a finite element approximation of $w_g \in H_0^1(\Omega)$ which uniquely solves

$$(3.1) \quad A(w_g, v) = (g, v), \quad \text{for all } v \in H_0^1(\Omega).$$

Set \mathcal{T} to be a subdivision of Ω made by simplices. We assume that \mathcal{T} is conforming (no hanging nodes) and shape-regular in a sense of [20, 14], i.e., there exists a positive constant c_{sr} so that for each cell $T \in \mathcal{T}$,

$$\text{diam}(T) \leq c_{\text{sr}} \rho_T$$

with $\text{diam}(T)$ and ρ_T denoting the size of T and the diameter of the largest ball inscribed in T , respectively. We also set $h_T = |T|^{1/d}$, with $|T|$ denoting the volume of T . So $h_T \sim \text{diam}(T)$, with the hiding constants depending on c_{sr} . Denote $\mathbb{V}(\mathcal{T}) \subset H_0^1(\Omega)$ the space of continuous piecewise linear functions subordinate to \mathcal{T} . So the finite element discretization for (3.1) reads: find $W_g \in \mathbb{V}(\mathcal{T})$ satisfying

$$(3.2) \quad A(W_g, V) = (g, V), \quad \text{for all } V \in \mathbb{V}(\mathcal{T}).$$

Given a subdivision \mathcal{T} , we call **GAL** the algorithm that returns the solution W_g to problem (3.2), summarized in Algorithm 3.1.

Algorithm 3.1 $W_g = \text{GAL}(\mathcal{T}, g)$

Solve $A(W_g, V) = (g, V)$, for all $V \in \mathbb{V}(\mathcal{T})$;

return W_g ;

3.2. A posteriori error estimates with $L^2(\Omega)$ data. AFEMs rely on the so-called computable error estimators to evaluate the quality of the finite element approximation on each cell T in the underlying subdivision \mathcal{T} . Here we consider the following local jump residual and data indicators: given a conforming subdivision \mathcal{T} , a finite element function $V \in \mathbb{V}(\mathcal{T})$ and a data function $g \in L^2(\Omega)$, we denote \mathcal{F}_T the collection of all faces of $T \in \mathcal{T}$ and define

$$(3.3) \quad j(V, T, \mathcal{T}) := \left(\sum_{F \in \mathcal{F}_T} h_F \| [A \cdot \nabla V] \|_{L^2(F)}^2 \right)^{1/2}$$

and

$$(3.4) \quad d(g, T, \mathcal{T}) := h_T \|g\|_{L^2(T)},$$

where h_F is the size of F and $[\cdot]$ denotes the normal jump across the face F . Their global counterparts are given by

$$\mathcal{J}(V, \mathcal{T}) := \left(\sum_{T \in \mathcal{T}} j(V, T, \mathcal{T})^2 \right)^{1/2} \quad \text{and} \quad \mathcal{D}(g, \mathcal{T}) := \left(\sum_{T \in \mathcal{T}} d(g, T, \mathcal{T})^2 \right)^{1/2}.$$

Letting $W_g = \text{GAL}(\mathcal{T}, g)$, we also define the local error indicator for the discrete problem (3.2):

$$e(W_g, T, \mathcal{T}) = (j(W_g, T, \mathcal{T})^2 + d(g, T, \mathcal{T})^2)^{1/2}$$

as well as the global indicator

$$\mathcal{E}(W_g, \mathcal{T}) = \left(\sum_{T \in \mathcal{T}} e(W_g, T, \mathcal{T})^2 \right)^{1/2}.$$

The computation of such indicators is usually performed in the stage **ESTIMATE** of AFEM algorithms, as summarized in Algorithm 3.2.

Algorithm 3.2 $\{j(T), d(T), e(T)\}_{T \in \mathcal{T}} = \text{ESTIMATE}(\mathcal{T}, W_g)$

Given the approximate solution W_g on \mathcal{T} ;

for $T \in \mathcal{T}$ **do**

 Compute $j(T) = j(W, T, \mathcal{T})$;

 Compute $d(T) = d(g, T, \mathcal{T})$;

 Compute $e(T) = e(W_g, T, \mathcal{T})$;

end for

return $\{j(T), d(T), e(T)\}_{T \in \mathcal{T}}$;

3.3. Marking of cells based on error indicators. The estimated error per cells obtained in the **ESTIMATE** algorithm are used to perform refinement based on the bulk chasing strategy [18] (or the Dörfler marking strategy), summarized in Algorithm 3.3. Here we set $\text{ind}(T)$ to be a local indicator and the corresponding global indicator is denoted by **IND**.

Algorithm 3.3 $\mathcal{M} = \text{MARK}(\{\text{ind}(T)\}_{T \in \mathcal{T}}, \mathcal{T}, \theta)$

Given a cell indicator $\{\text{ind}(T)\}_{T \in \mathcal{T}}$ and a bulk parameter $\theta \in (0, 1)$;

Find the smallest subset \mathcal{M} of \mathcal{T} satisfying

$$(3.5) \quad \left(\sum_{T \in \mathcal{M}} \text{ind}(T)^2 \right)^{1/2} \geq \theta \text{IND}.$$

return \mathcal{M} ;

3.4. Refinements of subdivisions. Starting from an initial subdivision \mathcal{T}_0 , we construct a sequence of conforming subdivisions $\{\mathcal{T}_k\}_{k=0}^{\infty}$ by adaptively refining some cells of \mathcal{T}_k satisfying Condition 3 (successive subdivisions), 4 (complexity of refinement) and 7 (admissible subdivision) in [11]. For conforming subdivisions of $\{\mathcal{T}_k\}$ in two dimensional case, the process of newest vertex bisection [6, 32] guarantees the above conditions. Eventually, we have

1. We bisect some marked cells $\mathcal{R}_k \subset \mathcal{T}_k$ once, together with minimal extra bisections to produce the conforming subdivision \mathcal{T}_{k+1} , i.e., $\mathcal{T}_k \subset \mathcal{T}_{k+1}$;
2. $\{\mathcal{T}_k\}$ are uniformly shape-regular, i.e., the constant c_{sr} is independent of k ;
3. The following complexity estimate holds: there exist a universal constant $C_{\text{com}} \geq 1$ satisfying

$$(3.6) \quad \#(\mathcal{T}_k) - \#(\mathcal{T}_0) \leq C_{\text{com}} \sum_{j=0}^{k-1} \#(\mathcal{R}_j).$$

For the process of newest vertex bisection for three dimensional case, we refer to [39]. Finally, we write the above refinement process from \mathcal{T}_k to \mathcal{T}_{k+1} as $\mathcal{T}_{k+1} = \text{REFINE}(\mathcal{T}_k, \mathcal{R}_k)$, summarized in Algorithm 3.4.

Algorithm 3.4 $\mathcal{T}_{k+1} = \text{REFINE}(\mathcal{T}_k, \mathcal{R}_k)$

Bisect the marked cells $\mathcal{R}_k \subset \mathcal{T}_k$ once;
 Add all extra bisections to produce a conforming subdivision \mathcal{T}_{k+1} ;
return \mathcal{T}_{k+1} ;

Remark 3.1. In what follows, our discussion only focuses on conforming triangular meshes. However, we point out that in Section 5 we will use regular (in the sense of [14]) quadrilateral subdivisions in 2d and hexahedral subdivisions in 3d to test our numerical algorithm, so that our finite element space is based on bilinear elements. To ensure the above refinement properties still holds, the sequence $\{\mathcal{T}_k\}$ is obtained from the quad-refinements strategy studied in [11], enforcing that each face in \mathcal{T}_k has at most one hanging node.

3.4.1. Overlay of two subdivisions. Providing that both \mathcal{T}_1 and \mathcal{T}_2 are refinements of \mathcal{T}_0 , we say that \mathcal{T} is the *overlay* of \mathcal{T}_1 and \mathcal{T}_2 when \mathcal{T} consists of the union of all cells of \mathcal{T}_1 that do not contain smaller cells of \mathcal{T}_2 and vice versa. Clearly, there holds

$$(3.7) \quad \#(\mathcal{T}) \leq \#(\mathcal{T}_1) + \#(\mathcal{T}_2) - \#(\mathcal{T}_0).$$

3.5. AFEM with control on L^2 data. It is well known (see e.g. [4, 19, 15]) that one can obtain a global upper and lower bound of the approximation error by the error indicator, i.e., there exist positive constants C_{rel} and C_{eff} so that

$$(3.8) \quad \|||w_g - W_g\||| \leq C_{\text{rel}} \mathcal{E}(W_g, \mathcal{T}),$$

and

$$(3.9) \quad \mathcal{E}(W_g, \mathcal{T}) \leq C_{\text{eff}} E(w_g, \mathcal{T})$$

with

$$(3.10) \quad E(w_g, \mathcal{T}) := (\|||w_g - W_g\|||^2 + \mathcal{D}(g, \mathcal{T})^2)^{1/2}.$$

We can also obtain a local version of (3.8): Let $\mathcal{M} \subset \mathcal{T}$ be the set of elements to be refined to construct \mathcal{T}^* . Denote W_g^* the discrete solution of (3.2) under the subdivision \mathcal{T}^* . Then there exists $C_L > C_{\text{rel}}$ so that

$$(3.11) \quad \|||W_g^* - W_g\||| \leq C_L \mathcal{E}(W_g, \mathcal{M}).$$

Remark 3.2 (Local lower bound with oscillation). The data indicator $\mathcal{D}(g, \mathcal{T})$ in (3.9) can be replaced by the data oscillation:

$$\text{osc}(g, \mathcal{T}) = \left(\sum_{T \in \mathcal{T}} h_T^2 \|g - a_T(g)\|_{L^2(T)}^2 \right)^{1/2},$$

where $a_T(\cdot)$ denotes the average on T . Note that $\text{osc}(g, \mathcal{T}) \leq \mathcal{D}(g, \mathcal{T})$, and the decay of the data oscillation could be faster if g is more regular. However, in our case, we

set $g = F^r$ to be as in definition 2.4, and the smoothness of g depends on the choice of ψ in Assumption 2.1. On the other hand, according to [12], the quasi-optimality of AFEMs using the linear element setting can still be achieved, even for $g \in L^2(\Omega)$, and we can drop the term $a_T(g)$ in the local lower bound.

Following the above remark, one should use the local L^2 data as an error indicator in the **MARK** stage before actually solving the problem (i.e., before calling **GAL**), and then trigger a **REFINE** step. We gather these steps in a **DATA** refinement stage, summarized in Algorithm 3.5.

Algorithm 3.5 $\mathcal{T}^* = \text{DATA}(\mathcal{T}, g, \tau^*, \tilde{\theta})$

```

while  $\mathcal{D}(g, \mathcal{T}) > \tau^*$  do
   $\mathcal{M} = \text{MARK}(\{d(g, T, \mathcal{T})\}_{T \in \mathcal{T}}, \mathcal{T}, \tilde{\theta});$ 
   $\mathcal{T} = \text{REFINE}(\mathcal{T}, \mathcal{M});$ 
end while
return  $\mathcal{T};$ 

```

3.6. AFEM algorithm for L^2 data. To summarize the above steps in a complete AFEM algorithm, we follow [15] to solve problem (3.1) by iteratively generating refined subdivisions and the corresponding finite element approximations. For convenience, we denote $W_k \in \mathbb{V}_k := \mathbb{V}(\mathcal{T}_k)$ the finite element approximation of W_g on \mathcal{T}_k . Similarly, we denote the local indicators $j_k(T) := j(W_k, T, \mathcal{T}_k)$, $d_k(T) := d(g, T, \mathcal{T}_k)$, $e_k(T) := e(W_k, T, \mathcal{T}_k)$ and global indicators $\mathcal{J}_k := \mathcal{T}(W_k, \mathcal{T}_k)$, $\mathcal{D}_k := \mathcal{D}(g, \mathcal{T}_k)$, $\mathcal{E}_k := \mathcal{E}(W_k, \mathcal{T}_k)$.

Starting from a conforming subdivision \mathcal{T}_0 and given a tolerance $\tau > 0$, we choose $\theta, \tilde{\theta}, \lambda \in (0, 1)$ and construct the approximation U_k by the routine **SOLVE**, defined in Algorithm 3.6.

Algorithm 3.6 $\{W^*, \mathcal{T}^*\} = \text{SOLVE}(\mathcal{T}_0, g, \tau, \theta, \tilde{\theta}, \lambda)$

```

 $W_0 = \text{GAL}(\mathcal{T}_0, g);$ 
 $\{j_0(T), d_0(T)\}_{T \in \mathcal{T}_0} = \text{ESTIMATE}(\mathcal{T}_0, W_0, g);$ 
 $k = 0;$ 
while  $\mathcal{E}_k > \tau$  do
   $\mathcal{M}_k = \text{MARK}(\{e_k(T)\}_{T \in \mathcal{T}_k}, \mathcal{T}_k, \theta);$ 
  if  $\mathcal{D}_k > \sigma_k := \lambda \theta \mathcal{E}_k$  then
     $\mathcal{T}_{k+1} = \text{DATA}(\mathcal{T}_k, g, \frac{\sigma_k}{2}, \tilde{\theta});$ 
  else
     $\mathcal{T}_{k+1} = \text{REFINE}(\mathcal{T}_k, \mathcal{M}_k);$ 
  end if
   $k = k + 1;$ 
   $W_k = \text{GAL}(\mathcal{T}_k, g);$ 
   $\{j_k(T), d_k(g, T)\}_{T \in \mathcal{T}_0} = \text{ESTIMATE}(\mathcal{T}_k, W_k, g);$ 
end while
return  $\{W_k, \mathcal{T}_k\};$ 

```

According to [15], the routine **SOLVE** guarantees the decay of the error indicator \mathcal{E}_k with some decay factor $\alpha \in (0, 1)$ (see also Theorem 4.4) and hence, when this

routine terminates, we obtain that

$$(3.12) \quad \|w_g - W_g\| \leq C_{\text{reg}}\tau.$$

Here we applied the upper bound (3.8) in above.

3.7. AFEM algorithm for regularized H^{-1} data. Let us first provide an assumption on the initial subdivision \mathcal{T}_0 related to the interface γ . Recalling that $\gamma \in C^2$ and denoting $p(x)$ the corresponding signed distance function, one can find a tubular expansion U_δ of width δ about γ so that the decomposition of $x \in U$

$$x = P(x) - d(x)\nabla p(x) \quad \text{with} \quad P(x) \in \gamma$$

is unique. To achieve this, letting $\mathbf{H} = \nabla^2 p$ be the Weingarten map and $\{\kappa_i\}_{i=1,\dots,d}$ be eigenvalues of \mathbf{H} , we require that $\delta < \min_{i=1,\dots,d} 1/\|\kappa_i\|_{L^\infty(\gamma)}$ (cf. [16, 17, 21]). Denoting

$$\mathcal{G} := \mathcal{G}(\gamma, \mathcal{T}) := \{T \in \mathcal{T} : T \cap \gamma \neq \emptyset\} \quad \text{and} \quad \text{diam}(\mathcal{G}) = \max_{T \in \mathcal{G}} h_T,$$

we assume that the initial subdivision satisfies

$$(3.13) \quad \mathcal{G}(\gamma, \mathcal{T}_0) \subset U_\delta.$$

Given a target tolerance $\tau > 0$, we shall determine the regularization parameter r and approximate problem (3.1) with $g = F^r$ via SOLVE so that the output approximation U satisfies

$$\|u - U\| \leq \|u - u^r\| + \|u^r - U\| \leq C_{\text{reg}}\tau.$$

To control $\|u - u^r\|$, in view of Proposition 2.7, we can set

$$m^{-1/2}C_{\text{rel}}r^{1/2}\|f\|_{L^2(\gamma)} \leq \frac{C_{\text{rel}}\tau}{2}.$$

Hence we choose the regularization parameter

$$(3.14) \quad r := r(\tau) := \left(\frac{C_{\text{rel}}\tau}{2C_{\text{reg}}\|f\|_{L^2(\gamma)}} \right)^2.$$

Remark 3.3 (values of the constants in (3.14)). Since it is non-trivial to compute the constants that appear in (3.14), in the simulations presented in Section 5 we select $r = \tau^2$.

From the computational point of view, if $r \ll h_T$ for $T \in \mathcal{G}(\gamma, \mathcal{T})$ and $V \in \mathbb{V}(\mathcal{T})$ is nonzero in T , it could be very hard to compute the quantity (F^r, V) using standard quadrature formula defined on T . In order to avoid such situation, we also refine the subdivision before controlling the error $\|u^r - U\|$ from SOLVE. Our goal is to find a refinement \mathcal{T}^* of \mathcal{T} so that

$$2 \text{diam}(\mathcal{G}(\gamma, \mathcal{T}^*)) \leq r.$$

To this end, we introduce the routine INTERFACE in Algorithm 3.7.

Algorithm 3.7 $\mathcal{T}^* = \text{INTERFACE}(\mathcal{T}, r)$

```

while  $\text{diam}(\mathcal{G}) > \frac{r}{2}$  do
   $\mathcal{M} = \text{INTERFACEMARK}(\mathcal{G}, \frac{r}{2});$ 
   $\mathcal{T} = \text{REFINE}(\mathcal{T}, \mathcal{M});$ 
end while
return  $\mathcal{T};$ 

```

Here the subroutine `INTERFACEMARK` marks all cells T of \mathcal{G} satisfying $h_T > \frac{r}{2}$, and it is summarized in Algorithm 3.8.

Algorithm 3.8 $\mathcal{M} = \text{INTERFACEMARK}(\mathcal{T}, r)$

```

Find the set  $\mathcal{M} := \{T \in \mathcal{G}(\gamma, \mathcal{T}) \text{ s.t. } h_T := \text{diam}(T) > \frac{r}{2}\};$ 
return  $\mathcal{M};$ 

```

Given an initial conforming subdivision \mathcal{T}_0 satisfying assumption (3.13), an initial tolerance τ_0 , and $\beta, \theta, \tilde{\theta}, \lambda, \tilde{\mu} \in (0, 1)$, the solver routine `REGSOLVE` for (2.5) reads as in Algorithm 3.9.

Algorithm 3.9 $\{U, \mathcal{T}\} = \text{REGSOLVE}(g, \mathcal{T}_0, j_{\max}, \tau_0, \beta, \theta, \tilde{\theta}, \lambda, \tilde{\mu})$

```

for  $j = 0 : j_{\max}$  do
   $r_j = r(\tau_j);$ 
   $\tilde{\mathcal{T}}_j = \text{INTERFACE}(\mathcal{T}_j, r_j);$ 
   $\{U_{j+1}, \mathcal{T}_{j+1}\} = \text{SOLVE}(\tilde{\mathcal{T}}_j, F^{r_j}, \tilde{\mu}\tau_j, \theta, \tilde{\theta}, \lambda);$ 
   $\tau_{j+1} = \beta\tau_j;$ 
   $j = j + 1;$ 
end for
return  $\{U_{j_{\max}}, \mathcal{T}_{j_{\max}}\};$ 

```

Here $\tilde{\mu}$ is a constant whose choice will be explained later in Lemma 4.14. Note that the subroutine `SOLVE` in `REGSOLVE` guarantees that the energy error between U and u^r is bounded by $\tilde{\mu}\tau_j$. Whence,

PROPOSITION 3.4. *Let u and U_j be defined as in (2.5) and `REGSOLVE`, respectively. Then for each nonnegative integer j ,*

$$\begin{aligned} \| \|u - U_{j+1}\| \| &\leq \| \|u - u^{r_j}\| \| + \| \|u^{r_j} - U_{j+1}\| \| \\ &\lesssim \| \|u - u^{r_j}\| \| + \mathcal{E}(u^{r_j}, \mathcal{T}_{j+1}) \lesssim \tau_j. \end{aligned}$$

Remark 3.5 (another algorithm). Since `INTERFACE` is an *a-priori* process, we can also solve (2.5) with only one iterate in `REGSOLVE`. That is

$$\{U, \mathcal{T}\} = \text{REGSOLVE}(g, \mathcal{T}_0, 1, \tau, \beta, \theta, \tilde{\theta}, \lambda, \tilde{\mu})$$

with $\tau = \tau_0\beta^{j_{\max}}$ denoting the final tolerance. So input argument β will be not be used in `REGSOLVE`.

4. Measuring the performance. In this section we measure the performance of `REGSOLVE`, i.e., we analyze the subroutines `INTERFACE` and `SOLVE` respectively. We use notation $::$ to connect a routine and its subroutine. For instance, the routine `SOLVE` in `REGSOLVE` is denoted by `REGSOLVE::SOLVE`.

4.1. Performance of INTERFACE.

PROPOSITION 4.1 (performance of INTERFACE). *Under assumption (3.13) for the initial subdivision \mathcal{T}_0 , given a refinement \mathcal{T} of \mathcal{T}_0 , let $\tilde{\mathcal{T}}$ be the output of the routine $\text{INTERFACE}(\mathcal{T}, r)$ with $r < 2 \text{diam}(\mathcal{G}(\gamma, \mathcal{T}_0))$. Then*

$$(4.1) \quad \#(\tilde{\mathcal{T}}) - \#(\mathcal{T}) \lesssim r^{1-d}.$$

Proof. Note that the marked cells in the routine $\text{INTERFACE}(\mathcal{T}, r)$ are also marked in $\mathcal{T}^* = \text{INTERFACE}(\mathcal{T}_0, r)$. So $\#(\tilde{\mathcal{T}}) - \#(\mathcal{T}) \leq \#(\mathcal{T}^*) - \#(\mathcal{T}_0)$ and it suffices to show that

$$\#(\mathcal{T}^*) - \#(\mathcal{T}_0) \lesssim r^{1-d}.$$

We split the proof in the following several steps.

1 For a fixed $T \in \mathcal{G}(\gamma, \mathcal{T}_0)$, denote \mathcal{G}_T^i the set of cells in the i -th full refinement of T that intersect with γ . For each $\tilde{T} \in \mathcal{G}_T^i$, $|\tilde{T}| = 2^{-i}|T|$. Letting $\gamma_T = \gamma \cap T$, due to the smooth assumption of γ , the tubular expansion of γ_T with width $2^{-i/d}|T|^{1/d}$ (i.e., the size of $\tilde{T} \in \mathcal{G}_T^i$) contains \mathcal{G}_T^i . That is

$$\sum_{\tilde{T} \in \mathcal{G}_T^i} |\tilde{T}| \lesssim 2^{-i/d}|T|^{1/d}|\gamma_T|.$$

Here the hidden constant in the above inequality only depends on γ . Whence,

$$\#(\mathcal{G}_T^i) \lesssim 2^{i(1-1/d)}|T|^{1/d-1}|\gamma_T|.$$

2 For each nonnegative integer j , let \mathcal{B}_j be the subset of $\mathcal{G}(\gamma, \mathcal{T}_0)$ such that for $T \in \mathcal{B}_j$,

$$(4.2) \quad 2^{-j-1}|U_\delta| \leq |T| \leq 2^{-j}|U_\delta|.$$

Since $\sum_{T \in \mathcal{B}_j} |T| \leq |U_\delta|$, we have $\#(\mathcal{B}_j) \leq 2^{j+1}$. On the other hand, there exists a positive integer j_r satisfying

$$(4.3) \quad 2^{-j_r-1}|U_\delta| \leq r^d \leq 2^{-j_r}|U_\delta|.$$

So for each $T \in \mathcal{B}_j$, we should bisect T at least $i := j_r - j + 1$ times to obtain \mathcal{G}_T^i satisfying $h_{\tilde{T}} \leq \frac{r}{2}$ based on the stop criteria of **INTERFACE**. According to Step 1, the cardinality of marked cells in T , denoting with \mathcal{R}_T , can be bounded by

$$\begin{aligned} \#(\mathcal{R}_T) &= \sum_{k=0}^i \#(\mathcal{G}_T^k) \lesssim \sum_{k=0}^i 2^{k(1-1/d)}|T|^{1/d-1}|\gamma_T| \\ &\leq 2^{(i+1)(1-1/d)}|T|^{1/d-1}|\gamma_T| \\ &\lesssim 2^{(j_r-j)(1-1/d)}|T|^{1/d-1}|\gamma_T| \lesssim 2^{j_r(1-1/d)}|U_\delta|^{1/d-1}|\gamma_T|. \end{aligned}$$

Here for the last inequality above we applied the left hand side of (4.2). Summing up the above estimate for all $T \in \mathcal{B}_j$ to get

$$\#(\mathcal{R}_j) := \sum_{T \in \mathcal{B}_j} \#(\mathcal{R}_T) \lesssim 2^{j_r(1-1/d)}|U_\delta|^{1/d-1}|\gamma_j|$$

with γ_j denoting the union of γ_T for $T \in \mathcal{B}_j$.

3 We continue to collect marked cells for all \mathcal{B}_j based on the result provided by Step 2. Since \mathcal{B}_j are pairwise disjoint and thanks to (3.6), we conclude that

$$\#(\mathcal{T}^*) - \#(\mathcal{T}_0) \lesssim 2^{j_r(1-1/d)} |U_\delta|^{1/d-1} |\gamma| \lesssim r^{1-d} |\gamma|,$$

where the last inequality above follows the right hand side of (4.3). The proof is complete. \square

Remark 4.2. The above estimate also holds when using quad-refinement for quads or hexes, as well as for piecewise C^2 interfaces γ , provided that the regions where γ has a regularity jump coincide with cell boundaries, that is, for each $T \in \mathcal{G}(\mathcal{T}_0, \gamma)$, $\gamma_T \in C^2$.

A direct application of Proposition 4.1 is to bound the cardinality of refined cells from INTERFACE in REGSOLVE.

COROLLARY 4.3 (performance of REGSOLVE::INTERFACE). *Let $\{\tilde{\mathcal{T}}_j\}$ be the sequence of subdivisions generated by INTERFACE in REGSOLVE. Then at j -th iterate, there exists a positive constant*

$$I_0 := I_0(c_{sr}, \gamma, f, \psi, C_{com})$$

satisfying

$$(4.4) \quad \#(\tilde{\mathcal{T}}_j) - \#(\mathcal{T}_j) \leq I_0 \tau_j^{-2(d-1)}.$$

Proof. The target estimate directly follows from (4.1) by the relation $r \sim \tau^2$. \square

4.2. Performance of SOLVE. We review some estimates for the complexity of SOLVE following the analysis from [15].

Contraction property. One instrumental tool to evaluate the performance of SOLVE is the following contraction property. The proof is similar to [15, Theorem 4.3]. For completeness, a detailed proof is provided in Appendix.

THEOREM 4.4 (contraction of SOLVE). *There exist two constants $\alpha \in (0, 1)$ and $\tilde{\alpha} > 0$ depending on c_{sr} , m , M , and on the bulk parameter θ in SOLVE such that for all $k \geq 0$,*

$$\|w_g - W_{k+1}\|^2 + \tilde{\alpha} \mathcal{E}(W_{k+1}, \mathcal{T}_{k+1})^2 \leq \alpha^2 \left(\|w_g - W_k\|^2 + \tilde{\alpha} \mathcal{E}(W_k, \mathcal{T}_k)^2 \right).$$

Approximation classes. We denote \mathcal{T}_n the set of all conforming subdivisions generated from \mathcal{T}_0 satisfying $\#(\mathcal{T}) \leq n$. Define the best error obtained in \mathcal{T}_n

$$\sigma_n(u)_{H_0^1(\Omega)} := \inf_{\mathcal{T} \in \mathcal{T}_n} \|u - U_{\mathcal{T}}\|$$

with $U_{\mathcal{T}} \in \mathbb{V}(\mathcal{T})$ be the Galerkin projection of u , i.e.,

$$A(U_{\mathcal{T}}, V) = \langle F, V \rangle_{H^{-1}(\Omega), H_0^1(\Omega)}, \quad \text{for all } V \in \mathbb{V}(\mathcal{T})$$

and it also satisfies that

$$\|u - U_{\mathcal{T}}\| = \inf_{V \in \mathbb{V}(\mathcal{T})} \|u - V\|.$$

Define the approximation class \mathcal{A}^s with $s \in (0, \frac{1}{d}]$ to be the set of all $v \in H_0^1(\Omega)$ such that the following quasi-semi-norm

$$|v|_{\mathcal{A}^s} := \sup_{n \geq 1} \left(n^s \sigma_n(v)_{H_0^1(\Omega)} \right)$$

is finite. If $d = 2$, noting that $u \in H^{1+s}(\Omega)$ for any $s \in (0, \frac{1}{d})$, Theorem 5.1 of [7] implies that $u \in \mathcal{A}^s$. A similar result should also apply for three dimensional problems.

Performance of DATA. The approximation class \mathcal{A}^s provides the rate of convergence for the energy error $\|u - U_{\mathcal{T}}\|$. Recalling that given $g \in L^2(\Omega)$, the total error $E(w_g, \mathcal{T})$ defined in (3.10) consists of both the energy error and the data indicator. So we are also concerned with the rate of convergence for the data indicator $\mathcal{D}(g, \mathcal{T})$. Here we assume that

Assumption 4.5. For $\tau > 0$, set $\mathcal{T}^* = \text{DATA}(\mathcal{T}, g, \tau)$. Then for $s \in (0, \frac{1}{d}]$, there exists a positive constant G_s (depends on g) satisfying

$$\#(\mathcal{T}^*) - \#(\mathcal{T}) \leq G_s \tau^{-1/s}.$$

Cardinality of refined cells in SOLVE. In the routine SOLVE, we need to estimate the cardinalities of \mathcal{M}_k as well as the cells refined from DATA. The latter comes from Assumption 4.5. The estimate of the former requires the following bulk property (cf. [15, Lemma 5.2]):

LEMMA 4.6. *Assume that the bulk parameter $\theta \in (0, \theta_*)$ with*

$$(4.5) \quad \theta_* = \frac{1}{C_{eff} \sqrt{1 + C_L^2}}.$$

Let \mathcal{T}^ be a refinement of \mathcal{T} and denote $\mathcal{R}_{\mathcal{T} \rightarrow \mathcal{T}^*}$ the set all refined cells from \mathcal{T} to \mathcal{T}^* . If $E(w_g, \mathcal{T}^*) \leq \xi E(w_g, \mathcal{T})$ with*

$$(4.6) \quad \xi := \sqrt{1 - \frac{\theta^2}{\theta_*^2}},$$

There holds $\mathcal{E}(W_g, \mathcal{R}_{\mathcal{T} \rightarrow \mathcal{T}^}) \geq \theta \mathcal{E}(W_g, \mathcal{T})$.*

Using Assumption 4.5 and the above lemma, Lemma 5.3 of [15] implies that for each iterate k in SOLVE, there holds that

$$(4.7) \quad \#(\mathcal{M}_k) \lesssim (|w_g|_{\mathcal{A}^s} + G_s)^{1/s} E(w_g, \mathcal{T}_k)^{-1/s}.$$

4.3. Performance of REGSOLVE. In this section, we shall adapt the results in the previous section to REGSOLVE.

4.3.1. Performance of DATA using F^r . To show that Assumption 4.5 holds for $g \in L^2(\Omega)$ with $s = \frac{1}{d}$, starting from a conforming initial subdivision \mathcal{T}_0 , we can construct an approximation of $g \in L^2(\Omega)$ using a greedy algorithm (see Algorithm 4.1).

According to [15, Theorem 7.3], there exists a positive constant K depending only on the shape regularity constant c_{sr} such that

$$\#(\mathcal{T}) - \#(\mathcal{T}_0) \leq K \|g\|_{L^2(\Omega)}^2 \tau^{-d}.$$

Algorithm 4.1 $\mathcal{T} = \text{GREEDY}(\mathcal{T}_0, g, \tau)$

```

 $\mathcal{T} = \mathcal{T}_0$ 
while  $\mathcal{D}(g, \mathcal{T}) > \tau$  do
   $T = \text{argmax}\{d(g, T, \mathcal{T})\};$ 
   $\mathcal{T} = \text{REFINE}(\mathcal{T}, \{T\});$ 
end while
return  $\mathcal{T};$ 

```

The above result can be extended by replacing \mathcal{T}_0 with its refinement \mathcal{T} , i.e., $\mathcal{T}^* = \text{GREEDY}(\mathcal{T}, g, \tau)$, and there holds

$$(4.8) \quad \#(\mathcal{T}^*) - \#(\mathcal{T}) \leq K \|g\|_{L^2(\Omega)}^2 \tau^{-d}.$$

This is because the marked cells in $\text{GREEDY}(\mathcal{T}, g, \tau)$ are contained in those generated by $\text{GREEDY}(\mathcal{T}_0, g, \tau)$; we refer to [10, Proposition 2] for a detailed discussion. Hence, any $L^2(\Omega)$ function g satisfies Assumption 4.5 with $s = \frac{1}{d}$ and $\|g\|_{L^2(\Omega)}^2 \sim G_{1/2}$. When $g = F^r$ as defined in Remark 2.5, the constant $G_{1/d}$ may still depend on r in an arbitrary refinement of \mathcal{T}_0 . However, the refinement process in DATA is based on the subdivisions generated by INTERFACE. So cells marked in GREEDY should be located in a neighborhood of a tubular extension of γ , whose width can be controlled by the regularization parameter r . In order to see the dependence of (4.8) on r , we modify the argument of Lemma 7.3 of [15].

LEMMA 4.7 (approximation class for F^r). *Assume that $f \in L^\infty(\gamma)$ and F^r is defined as in Remark 2.5 for any $r > 0$. Letting the initial subdivision \mathcal{T}_0 satisfy (3.13), we define $\tilde{\mathcal{T}} = \text{INTERFACE}(\mathcal{T}_0, r)$ with $r < c_\gamma$. For any $\tau > 0$, the cardinality of refined cells in $\mathcal{T}^* = \text{GREEDY}(\tilde{\mathcal{T}}, F^r, \tau)$ can be bounded by*

$$\#(\mathcal{T}^*) - \#(\tilde{\mathcal{T}}) \leq K_0 r^{1-d/2} \|f\|_{L^\infty(\gamma)}^d \tau^{-d},$$

where the constant K_0 is independent of r and τ . This implies that Assumption 4.5 holds for F^r with $s = \frac{1}{2}$ and $G_{1/2} \sim r^{1-d/2} \|f\|_{L^\infty(\gamma)}^d$ when $\mathcal{T} = \tilde{\mathcal{T}}$.

Proof. We split the proof in the following steps.

[1] Suppose that there are totally N iterations executed in the while loop when $\text{GREEDY}(\tilde{\mathcal{T}}, F^r, \tau)$ terminates. We denote with $\{T^i\}_{i=0}^N$ the marked cells in the sequence and set $\mathcal{T}^i = \text{REFINE}(\mathcal{T}^{i-1}, \{T^{i-1}\})$ for $i = 1, \dots, N$ and $\mathcal{T}^0 = \tilde{\mathcal{T}}$. Let

$$\delta := d(F^r, T^{N-1}, \mathcal{T}^{N-1}) = \text{argmax}\{d(F^r, T, \mathcal{T}^{N-1}) : T \in \mathcal{T}^{N-1}\}.$$

Noting that for $0 \leq i \leq N-1$, there exists $T^i \in \mathcal{T}^i$ such that $T^{N-1} \subset T^i$. Clearly, by the definition of T^i , we have

$$(4.9) \quad d(F^r, T^i, \mathcal{T}^i) \geq d(F^r, T^i, \mathcal{T}^i) \geq d(F^r, T^{N-1}, \mathcal{T}^{N-1}) = \delta.$$

According to the definition of T^{N-1} , we also get

$$(4.10) \quad \tau \leq \mathcal{D}(F^r, \mathcal{T}^{N-1}) \leq \delta \sqrt{\#(T^{N-1})}.$$

[2] Since F^r is supported in U_r , $T^i \subset U_{cr}$ for some constant $c \geq 1$ depending on c_{sr} . Let $\mathcal{B}_j \subset \{T^i\}$ be the set satisfying

$$(4.11) \quad 2^{-(j+1)} |U_{cr}| < |T^i| \leq 2^{-j} |U_{cr}|, \quad j \geq 0.$$

Due to the refinement process from \mathcal{T}^i to \mathcal{T}^{i+1} , $\{T^i\}$ are distinct from each other. This implies that by summing up the first inequality of (4.11) for all $T^i \in \mathcal{B}_j$, we obtain $\#\mathcal{B}_j < 2^{j+1}$. using the second inequality of (4.11) as well as (4.10), we realize that for $T^i \in \mathcal{B}_j$,

$$\delta \leq d(F^r, T^i, \mathcal{T}^i) = |T^i|^{1/d} \|F^r\|_{L^2(T^i)} \leq 2^{-j/d} |U_{cr}|^{1/d} \|F^r\|_{L^2(T^i)}.$$

We square the above estimate and sum it up for all $T^i \in \mathcal{B}_j$ to obtain

$$\delta^2 \#\mathcal{B}_j \leq 2^{-2j/d} |U_{cr}|^{2/d} \|F^r\|_{L^2(U_{cr})}^2$$

The above estimate together with $\#\mathcal{B}_j < 2^{j+1}$ implies that the total marked cells can be estimated with

$$(4.12) \quad N = \sum_{j \geq 0} \#\mathcal{B}_j \leq \sum_{j \geq 0} \min(2^{-2j/d} \delta^{-2} |U_{cr}|^{2/d} \|F^r\|_{L^2(U_{cr})}^2, 2^{j+1}).$$

3 Since the first term of the above minimum decreases with respect to j , we set j_0 be the smallest integer such that

$$(4.13) \quad 2^{j_0+1} > 2^{-2j_0/d} \delta^{-2} |U_{cr}|^{2/d} \|F^r\|_{L^2(U_{cr})}^2.$$

Simplifying this relation for j_0 we get

$$2^{-j_0} \lesssim \left(\delta^{-1} |U_{cr}|^{1/d} \|F^r\|_{L^2(U_{cr})} \right)^{-2d/(2+d)}.$$

If $j_0 > 0$, (4.13) is violated for $j = j_0 - 1$ and we can deduce that

$$2^{j_0} \lesssim \left(\delta^{-1} |U_{cr}|^{1/d} \|F^r\|_{L^2(U_{cr})} \right)^{2d/(2+d)}.$$

Inserting the above two estimate in (4.12), we have

$$(4.14) \quad \begin{aligned} N &\leq \sum_{j < j_0} 2^{j+1} + \delta^{-2} |U_{cr}|^{2/d} \|F^r\|_{L^2(U_{cr})}^2 \sum_{j \geq j_0} 2^{-2j/d} \\ &\lesssim 2^{j_0} + \left(\delta^{-1} |U_{cr}|^{1/d} \|F^r\|_{L^2(U_{cr})} \right)^2 2^{-2j_0/d} \\ &\lesssim \left(\delta^{-1} |U_{cr}|^{1/d} \|F^r\|_{L^2(U_{cr})} \right)^{2d/(2+d)} \end{aligned}$$

4 We shall further bound the above estimate by considering the $L^2(U_{cr})$ -norm of F^r . In fact,

$$\begin{aligned} \|F^r\|_{L^2(U_{cr})}^2 &= \int_{U_{cr}} \left(\int_{\gamma} \delta^r(x-y) f(y) dy \right)^2 dx \\ &\leq \frac{1}{r^{2d}} \|\psi\|_{L^\infty(\mathbb{R}^d)}^2 \|f\|_{L^\infty(\gamma)}^2 \int_{U_{cr}} |B_r(x) \cap \gamma|^2 dx \\ &\leq C \frac{1}{r^{2d}} \|\psi\|_{L^\infty(\mathbb{R}^d)}^2 \|f\|_{L^\infty(\gamma)}^2 r^{2(d-1)+1} \lesssim r^{-1} \|f\|_{L^\infty(\gamma)}^2, \end{aligned}$$

where for the second inequality above we used the fact that $|B_r(x) \cap \gamma| \lesssim r^{d-1}$ for $x \in D_{cr}$ and $|D_{cr}| \sim |\gamma|r$.

5 Combining the results from Step 3 and 4 to deduce that

$$(4.15) \quad N \lesssim \delta^{-2d/(2+d)} r^{(2-d)/(2+d)} \|f\|_{L^\infty(\gamma)}^{2d/(2+d)},$$

where the hidden constant above depends on c_{sr}, γ, d and ψ . On the other hand, the complexity assumption (3.6) implies that

$$\#(\mathcal{T}^{N-1}) - \#(\mathcal{T}^0) \leq C_{\text{com}} N.$$

Hence the above relation together with (4.15) and (4.10) concludes that

$$\begin{aligned} \tau &\leq \delta \sqrt{\#(\mathcal{T}^{N-1})} \\ &\lesssim \frac{\sqrt{\#(\mathcal{T}^0) + C_{\text{com}} N}}{N^{(2+d)/(2d)}} r^{1/d-1/2} \|f\|_{L^\infty(\gamma)} \lesssim N^{-1/d} r^{1/d-1/2} \|f\|_{L^\infty(\gamma)}, \end{aligned}$$

which implies the target estimate.

6 If $j_0 = 0$, we directly get $\delta^{-1} |U_{cr}|^{1/d} \|F^r\|_{L^2(U_{cr})} \lesssim 1$. Starting from (4.12), we apply the result in Step 4 to write

$$\begin{aligned} N &\lesssim \delta^{-2} |U_{cr}|^{2/d} \|F^r\|_{L^2(U_{cr})}^2 \sum_{j \geq 0} 2^{-2j/d} \\ &\lesssim \delta^{-2} |U_{cr}|^{2/d} \|F^r\|_{L^2(U_{cr})}^2 \\ &\lesssim \delta^{-1} |U_{cr}|^{1/d} \|F^r\|_{L^2(U_{cr})} \lesssim \delta^{-1} r^{1/d-1/2} \|f\|_{L^\infty(\gamma)}. \end{aligned}$$

Therefore, we again obtain the target estimate following the argument in Step 5. The proof is complete. \square

Remark 4.8. Following the proof of [10, Proposition 2], we can extend the results in Lemma 4.7 by replacing $\tilde{\mathcal{T}}$ with any of its refinements. More precisely speaking, let \mathcal{T}^+ be any refinement of $\tilde{\mathcal{T}}$, and $\mathcal{T}^* = \text{GREEDY}(F^r, \mathcal{T}^+, \tau)$. Then,

$$\#(\mathcal{T}^*) - \#(\mathcal{T}^+) \lesssim r^{1-d/2} \|f\|_{L^\infty(\gamma)}^d \tau^{-d}.$$

Now we are ready to verify Assumption 4.5 when $g = F^r$ and \mathcal{T} is any refinement of $\text{INTERFACE}(\mathcal{T}_0, r)$. The proof follows [15, Theorem 7.5] using a contraction property of $\mathcal{D}(F^r, \mathcal{T})$, a bulk property and Lemma 4.7. For completeness, we provide a detailed proof in Appendix.

COROLLARY 4.9 (performance of DATA). *Under the assumptions provided by Lemma 4.7, Assumption 4.5 holds with $s = \frac{1}{d}$ and $g = F^r$ starting from $\tilde{\mathcal{T}} = \text{INTERFACE}(\mathcal{T}_0, r)$. Precisely speaking, given a refinement \mathcal{T} of $\tilde{\mathcal{T}}$, let \mathcal{T}^* be the output of $\text{DATA}(\mathcal{T}, F^r, \tau)$. Then, there exists a constant $K_0 > 0$ not depending on r or τ satisfying*

$$\#(\mathcal{T}^*) - \#(\mathcal{T}) \leq K_0 r^{1-d/2} \tau^{-d}.$$

4.3.2. Quasi-monotonicity of the data indicator. The following lemma provides a quasi-monotonicity of $\mathcal{D}(F^r, \mathcal{T})$ with respect to r . We note that this property relies on the forcing data f and nonnegativity of δ^r .

LEMMA 4.10. *Given $r_2 < r_1$, let \mathcal{T} be a refinement of $\text{INTERFACE}(\mathcal{T}_0, r_2)$. Then there holds that*

$$\mathcal{D}(F^{r_2}, \mathcal{T}) \lesssim \tilde{\beta}^{-d} \mathcal{D}(F^{r_1}, \mathcal{T}) + r_2,$$

where $\tilde{\beta} = r_2/r_1$.

Proof. We recall from the configuration of f in Section 2 that the set I separates the sign of f in γ . Define

$$\mathcal{B} := \{T \in \mathcal{T} : T \cap B_{r_2}(x_0) \neq \emptyset \text{ for some } x_0 \in I\}.$$

So,

$$(4.16) \quad \sum_{T \in \mathcal{B}} |T| \lesssim \frac{1}{r_2^{d-2}}.$$

Now we bound $d(F^{r_2}, T, \mathcal{T})$. If $T \notin \mathcal{B}$, since δ^r is nonnegative, we have $\delta^{r_2} \leq \tilde{\beta}^{-2d} \delta^{r_1}$. Hence,

$$d(F^{r_2}, T, \mathcal{T}) \leq \tilde{\beta}^{-d} d(F^{r_1}, T, \mathcal{T}).$$

If $T \in \mathcal{B}$, there holds

$$\begin{aligned} d(F^{r_2}, T, \mathcal{T})^2 &= h_T^2 \int_T \left(\int_\gamma f(y) \delta^{r_2}(y-x) \right)^2 dx \\ &\lesssim \frac{h_T^2}{r_2^{2d}} \int_T |B_{r_2}(x) \cap \gamma|^2 dx \\ &\lesssim \frac{h_T^2}{r_2^d} h_T^d r_2^{2(d-1)} \lesssim r_2^d \end{aligned}$$

where for the last inequality, we used the fact the $h_T \lesssim r_2$ according to Step 2 of the proof of Lemma 4.7. By summing up all contributions above and invoking (4.16), we arrive at

$$\begin{aligned} \mathcal{D}(F^{r_2}, \mathcal{T})^2 &= \sum_{T \in \mathcal{B}} d(F^{r_2}, T, \mathcal{T})^2 + \sum_{T \notin \mathcal{B}} d(F^{r_2}, T, \mathcal{T})^2 \\ &\lesssim \sum_{T \in \mathcal{B}} r_2^d + \sum_{T \notin \mathcal{B}} \tilde{\beta}^{-2d} d(F^{r_1}, T, \mathcal{T})^2 \\ &\lesssim r_2^2 + \tilde{\beta}^{-2d} \mathcal{D}(F^{r_1}, \mathcal{T}), \end{aligned}$$

which concludes the proof. \square

Remark 4.11. If f is nonnegative or non-positive along γ , according to the proof of Lemma 4.10, we immediately get

$$\mathcal{D}(F^{r_2}, \mathcal{T}) \leq \tilde{\beta}^{-d} \mathcal{D}(F^{r_1}, \mathcal{T}).$$

4.3.3. Performace of each subroutine in REGSOLVE. In terms of the approximation class for u^r , Lemma 3.2 of [10] enlightens us to exploit the fact that u^r is an approximation of u and then to characterize approximation properties of u^r with the approximation class of u , i.e., using the quasi-semi-norm $|u|_{\mathcal{A}^s}$ with any $s \in (0, \frac{1}{d})$.

LEMMA 4.12 (Lemma 3.2 of [10]). *If $\|u - u^r\| < \varepsilon$ for some $\varepsilon > 0$, then u^r is a 2ε -approximation to u of order s : for all $\delta > 2\varepsilon$, there exists a positive integer n such that*

$$\sigma_n(u^r)_{H_0^1(\Omega)} \leq \delta, \quad \text{and} \quad n \lesssim |u|_{\mathcal{A}^s}^{1/s} \delta^{-1/s}.$$

LEMMA 4.13 (a priori asymptotic decay of the total error). *Under the settings in Lemma 4.7, we set $r = r(\tau)$ according to (3.14) so that $\|u - u^r\| \leq C_{\text{rel}}\tau/2$ for some $\tau > 0$. Then for any $1 > \delta \geq \sqrt{2}C_{\text{rel}}\tau$, there is a conforming refinement \mathcal{T} of $\tilde{\mathcal{T}} = \text{INTERFACE}(\mathcal{T}_0, r)$ such that*

$$E(u^r, \mathcal{T}) \leq \delta \quad \text{and} \quad \#(\mathcal{T}) - \#(\tilde{\mathcal{T}}) \lesssim (K_0 r^{1-d/2} + |u|_{\mathcal{A}^s}^{1/s}) \delta^{-1/s}.$$

Proof. We denote $\mathcal{T}_f^r = \text{DATA}(\tilde{\mathcal{T}}, F^r, \delta/\sqrt{2})$. In view of Corollary 4.9, there holds

$$\mathcal{D}(F^r, \mathcal{T}_f^r) \leq \frac{\delta}{\sqrt{2}} \quad \text{and} \quad \#(\mathcal{T}_f^r) - \#(\tilde{\mathcal{T}}) \leq K_0 r^{1-d/2} \delta^{-1/s}.$$

On the other hand, Lemma 4.12 implies that there exists a subdivision \mathcal{T}_u^r so that

$$\|u^r - U_{\mathcal{T}_u^r}\| \leq \frac{\delta}{\sqrt{2}} \quad \text{with} \quad \#(\mathcal{T}_u^r) - \#(\mathcal{T}_0) \lesssim |u|_{\mathcal{A}^s}^{1/s} \delta^{-1/s}.$$

Now we let \mathcal{T} be the overlay of \mathcal{T}_f^r and \mathcal{T}_u^r . So \mathcal{T} is a refinement of $\tilde{\mathcal{T}}$ and we immediately get $E(u^r, \mathcal{T}) \leq \delta$. using the above estimates and in view of (3.7), we also get

$$\#(\mathcal{T}) - \#(\tilde{\mathcal{T}}) \leq (\#(\mathcal{T}_u^r) - \#(\mathcal{T}_0)) + (\#(\mathcal{T}_f^r) - \#(\tilde{\mathcal{T}})) \lesssim (K_0 r^{1-d/2} + |u|_{\mathcal{A}^s}^{1/s}) \delta^{-1/s}$$

as desired. \square

The next lemma provides the estimate of marked cells in SOLVE.

LEMMA 4.14 (cardinality of REGSOLVE::SOLVE::MARK). *Under the settings given by Lemma 4.7, let the bulk parameter θ defined in SOLVE satisfy the condition $\theta < \theta_*$, with θ_* provided by (4.5). For a fixed $\tau > 0$, set $r = r(\tau)$ in (3.14) and $\tilde{\mathcal{T}} = \text{INTERFACE}(\mathcal{T}_0, r)$. We also let $\{\mathcal{T}_k\}$ be defined in $\text{SOLVE}(\tilde{\mathcal{T}}, F^r, \tilde{\mu}\tau)$ with $\tilde{\mu} \geq \sqrt{2}C_{\text{rel}}/(\xi C_{\text{eff}})$ and $\{\mathcal{M}_k\}$ be the set of marked cells generated from $\text{SOLVE}::\text{MARK}$ at \mathcal{T}_k . Then there holds*

$$\#(\mathcal{M}_k) \lesssim (K_0 r^{1-d/2} + U_s) E(u^r, \mathcal{T}_k)^{-1/s},$$

where $U_s := |u|_{\mathcal{A}^s}^{1/s}$.

Proof. We define $\epsilon = \xi E(u^r, \mathcal{T}_k)$, recalling that ξ is given by (4.6). Since the target tolerance of SOLVE is $\tilde{\mu}\tau$, we have that $\epsilon \geq C_{\text{eff}}\xi\tilde{\mu}\tau \geq \sqrt{2}C_{\text{rel}}\tau$. In view of Lemma 4.13, there exists a conforming subdivision \mathcal{T}^ϵ so that $E(u^r, \mathcal{T}^\epsilon) \leq \epsilon$ and

$$\#(\mathcal{T}^\epsilon) - \#(\tilde{\mathcal{T}}) \lesssim (K_0 r^{1-d/2} + U_s) \epsilon^{-1/s}.$$

Now let \mathcal{T}^* be the overlay of \mathcal{T}^ϵ and \mathcal{T}_k . So \mathcal{T}^* is a refinement of \mathcal{T}^ϵ . This implies that $E(u^r, \mathcal{T}^*) \leq \epsilon = \xi E(u^r, \mathcal{T}_k)$, which satisfies the bulk property in Lemma 4.6. By the minimal assumption of \mathcal{M}_k , there holds that

$$\#(\mathcal{M}_k) \leq \#(\mathcal{R}_{\mathcal{T}_k \rightarrow \mathcal{T}^*}) \lesssim \#(\mathcal{T}^*) - \#(\mathcal{T}_k)$$

Since both \mathcal{T}_k and \mathcal{T}^* are refinements of $\tilde{\mathcal{T}}$, invoking (3.7) with respect to $\tilde{\mathcal{T}}$, we also have

$$\#(\mathcal{T}^*) \leq \#(\mathcal{T}^\epsilon) + \#(\mathcal{T}_k) - \#(\tilde{\mathcal{T}}).$$

We continue to bound $\#(\mathcal{M}_k)$ by

$$\#(\mathcal{M}_k) \lesssim \#(\mathcal{T}^\epsilon) - \#(\tilde{\mathcal{T}}) \lesssim (K_0 r^{1-d/2} + U_s) \epsilon^{-1/s} \lesssim (K_0 r^{1-d/2} + U_s) E(u^r, \mathcal{T}_k)^{-1/s}.$$

The proof is complete. \square

LEMMA 4.15 (performance of REGSOLVE::SOLVE). *Denote $\{(\mathcal{T}_j, U_j)\}_{j=0}^{j_{\max}}$ to be the sequence of subdivisions and approximations of u generated by REGSOLVE, respectively. Under the assumptions provided by Lemma 4.7 and Lemma 4.14, there holds that for $j \geq 1$,*

$$\#(\mathcal{T}_j) - \#(\tilde{\mathcal{T}}_j) \lesssim (K_0 r^{1-d/2} + U_s) \tau_j^{-1/s}$$

Proof. For each $j \geq 1$, we let k_{\max} be the number of iterations executed in SOLVE. Let us first show that k_{\max} is uniform bound with respect to j . Let $\hat{\tau}_j$ be the error indicator for $\tilde{U}_j = \text{GAL}(\tilde{\mathcal{T}}_j, F^{r_j})$ with $r_j = r(\tau_j)$ in REGSOLVE. In view of (3.9), (3.8) and Lemma 4.10, we have

$$\begin{aligned} \hat{\tau}_j &\lesssim E(u^{r_j}, \tilde{\mathcal{T}}_j) \lesssim \left\| \|u^{r_j} - \tilde{U}_j\| \right\| + \mathcal{D}(F^{r_j}, \tilde{\mathcal{T}}_j) \\ &\lesssim \|u^{r_j} - U_j\| + \mathcal{D}(F^{r_{j-1}}, \tilde{\mathcal{T}}_j) + r_j \\ &\leq \|u - u^{r_j}\| + \|u - U_j\| + \mathcal{D}(F^{r_{j-1}}, \mathcal{T}_j) + r_j \\ &\lesssim \|u - u^{r_j}\| + \|u - U_j\| + \mathcal{E}(u^{r_{j-1}}, \mathcal{T}_j) + r_j \end{aligned}$$

Now we invoke Proposition 3.4 and 2.7 to deduce

$$(4.17) \quad \hat{\tau}_j \lesssim r_j^{1/2} + \tau_{j-1} + r_j \lesssim \tau_j + \tau_{j-1} \lesssim \tau_j.$$

Here in the above estimates we also used the relations $r_j \lesssim \tau_{j+1}^2$ and $\tau_j = \beta \tau_{j-1}$. The contraction property (4.4) together with (4.17) yields the uniform boundedness of k_{\max} .

At each iteration $k = 0, 1, \dots, k_{\max}$ in SOLVE, Lemma 4.14 controls the number of marked cells in REFINE. For the cardinality of the marked cells in DATA, we set \mathcal{T}_k^+ to be the corresponding output and apply Corollary 4.9 to get,

$$\#(\mathcal{T}_k^+) - \#(\mathcal{T}_k) \lesssim K_0 r^{1-d/2} (\lambda \theta \mathcal{E}_k)^{-1/s} \lesssim K_0 r^{1-d/2} E(u^r, \mathcal{T}_k)^{-1/s}.$$

Combing the above estimate together with Lemma 4.14, we obtain that

$$(4.18) \quad \begin{aligned} \#(\mathcal{T}_{j+1}) - \#(\tilde{\mathcal{T}}_j) &\lesssim \sum_{k=0}^{k_{\max}} (\#\mathcal{M}_k + \#(\mathcal{T}_k^+) - \#(\mathcal{T}_k)) \\ &\lesssim (r^{1-d/2} K_0 + U_s) \sum_{k=0}^{k_{\max}-1} E(u^r, \mathcal{T}_k)^{-1/s}. \end{aligned}$$

In view of Theorem 4.4, there holds that for $k \leq k_{\max}$,

$$E(u^r, \mathcal{T}_k) \lesssim \alpha^{k_{\max}-k} E(u^r, \mathcal{T}_k).$$

We apply the above relation into (4.18) to yield

$$\begin{aligned} \#(\mathcal{T}_{j+1}) - \#(\tilde{\mathcal{T}}_j) &\lesssim (K_0 r^{1-d/2} + U_s) E(u^r, \mathcal{T}_{k_{\max}})^{-1/s} \sum_{k=0}^{k_{\max}} \alpha^{(k_{\max}-k)/s} \\ &\lesssim (K_0 r^{1-d/2} + U_s) \tau^{-1/s}, \end{aligned}$$

where for the last inequality above we used the fact that $\tau \lesssim E(u^r, \mathcal{T}_{k_{\max}})$ and $\sum_{k=0}^{k_{\max}} \alpha^{(k_{\max}-k)/s} \leq \sum_{k=0}^{\infty} \alpha^{k/s} \lesssim 1$. The proof is complete. \square

4.3.4. Performance of REGSOLVE. We are now in a position to show our main result.

THEOREM 4.16 (performance of REGSOLVE). *Denote $\{(\mathcal{T}_j, U_j)\}_{j=0}^{j_{\max}}$ to be the sequence of subdivisions and approximations of u generated by REGSOLVE, respectively. Under the assumptions provided by Lemma 4.7 and Lemma 4.14, there holds that*

$$\#(\mathcal{T}_{j_{\max}}) - \#(\mathcal{T}_0) \lesssim (K_0 + I_0 + U_s) \tau_{j_{\max}}^{2-d-1/s}.$$

Proof. Denote \mathcal{M}_j the collections cells marked in the j -th iteration of solve. Invoking Corollary 4.3 and Lemma 4.15, we have

$$\begin{aligned} \#(\mathcal{M}_j) &= (\#(\tilde{\mathcal{T}}_j) - \#(\mathcal{T}_j)) + (\#(\mathcal{T}_{j+1}) - \#(\tilde{\mathcal{T}}_j)) \\ &\lesssim (I_0 \tau_j^{2-d} + K_0 \tau_j^{2-d} + U_s) \tau_j^{-1/s} \lesssim (I_0 + K_0 + U_s) \tau_j^{2-d-1/s}, \end{aligned}$$

where we used the setting $r \sim \tau_j^2$ according to (3.14). Summing up the above estimate for $j = 0, \dots, j_{\max} - 1$ and using the relation $\tau_{j_{\max}} = \beta^{j_{\max}-j} \tau_j$, we arrive at

$$\begin{aligned} \#(\mathcal{T}_j) - \#(\mathcal{T}_0) &= \sum_{j=0}^{j_{\max}-1} \#(\mathcal{M}_j) \\ &\lesssim (I_0 + K_0 + U_s) \tau_{j_{\max}}^{2-d-1/s} \sum_{j=0}^{j_{\max}-1} \beta^{(j_{\max}-j)(1/s+d-2)} \\ &\lesssim (I_0 + K_0 + U_s) \tau_{j_{\max}}^{2-d-1/s}, \end{aligned}$$

which is our target estimate. \square

Remark 4.17 (convergence rates). We can also bound the energy error at each iterate of REGSOLVE with respect to the number of degrees of freedom using the performance estimate in Theorem 4.16. In two dimensional space, we guarantee that the adaptive method is quasi-optimal, i.e.,

$$\| \|u - U_j\| \| \lesssim (\#(\mathcal{T}_j) - \#(\mathcal{T}_0))^{-1/2},$$

However, in three dimensional space, we have,

$$\| \|u - U_j\| \| \lesssim (\#(\mathcal{T}_j) - \#(\mathcal{T}_0))^{-1/4},$$

which turns out to be sub-optimal compared with the optimal rate $\frac{1}{3}$.

5. Numerical illustration. In this section, we test our numerical algorithm proposed in Section 3 for the following interface problem: letting γ be defined as in (2.1), we want to find u satisfying

$$(5.1) \quad \begin{aligned} -\Delta u &= 0, & \text{in } \Omega \setminus \gamma, \\ [u] &= 0, & \text{on } \gamma, \\ [\nabla u \cdot \nu_\gamma] &= f, & \text{on } \gamma, \\ u &= g, & \text{on } \partial\Omega, \end{aligned}$$

where $[\cdot]$ denotes the jump of the function across the interface and ν_γ is the outward normal direction along γ . So u satisfies the weak formulation (2.5) with the forcing data F defined by (2.3) and a non-homogeneous boundary condition.

As we mentioned in Section 3.4, our numerical implementation relies on the `deal.II` finite element library [3] (version 9.2) which uses quadrilateral subdivisions in two dimensions and hexahedral subdivisions in three dimensions. For the computation of the right hand side of the discrete system, we refer to Remark 22 of [26] for more details. In the following numerical simulations, we will use following types of ψ to compute Dirac delta approximations:

- *Radially symmetric C^1* : use (2.9) with $\psi_\rho(x) = c_d(1 + \cos(|\pi x|))\chi(x)$, where $\chi(x)$ is the characteristic function on the unit ball and c_d is a normalization constant so that $\int_{\mathbb{R}^d} \psi_\rho = 1$;
- *Tensor product C^1* : use (2.10) with $\psi_{1d}(x) = (1 + \cos(|\pi x|))\chi_{(-1,1)}(x)/2$;
- *Tensor product C^∞* : use (2.10) with $\psi_{1d}(x) = e^{1-1/(1-|x|^2)}\chi_{(-1,1)}(x)$;
- *Tensor product L^∞* : use (2.10) with $\psi_{1d}(x) = \frac{1}{2}\chi_{(-1,1)}(x)$.

In `REGSOLVE`, we fix $\tilde{\mu} = \frac{1}{2}$. The parameters \mathcal{T}_0 (initial subdivision), τ_0 (initial tolerance), β (tolerance reduction), j_{\max} (number of iterations), λ (ratio of PDE to DATA error balance), and the bulk parameters θ and $\tilde{\theta}$ will be provided for each numerical test. For the regularization parameter, we simply set $r(\tau_j) = \tau_j^2$ in `REGSOLVE::INTERFACE` to avoid the estimate of the constants C_{reg} , C_{rel} and $\|f\|_{L^2(\gamma)}$ in (3.14). Furthermore, after the last iteration of `REGSOLVE`, we perform the following extra steps

$$\begin{aligned} r_{j+1} &= r(\tau_{j_{\max}+1}); \\ \tilde{\mathcal{T}}_{j_{\max}+1} &= \text{INTERFACE}(\mathcal{T}_{j_{\max}+1}, r_{j+1}); \\ \text{GAL}(\tilde{\mathcal{T}}_{j_{\max}+1}, F^{r_{j+1}}); \end{aligned}$$

5.1. Convergence tests on a L-shaped domain. Following similar test cases to those presented in [27], we set $\Omega = (-1, 1)^2 \setminus [0, 1]^2$, $\gamma = \partial B_R(c)$ with $R = 0.2$ and $c = (0.5, -0.5)^T$, $f = \frac{1}{R}$ and $g = \ln(|x - c|)$. The analytic solution is

$$u(x) = r(x)^{2/3} \sin\left(\frac{2}{3}\left(\theta(x) - \frac{\pi}{2}\right)\right) + \begin{cases} -\ln(|x - c|), & \text{if } |x - c| > R, \\ -\ln(R), & \text{if } |x - c| \leq R \end{cases}$$

We start with an initial uniform grid \mathcal{T}_0 with the mesh size $\sqrt{2}/4$. Note that we also approximate the interface γ with a uniform subdivision whose vertices lie on γ . The corresponding mesh size is fixed as $2\pi R/2^{14}$ so that the geometric error will not dominate the total error. For the parameters showing the numerical algorithm, we set $j_{\max} = 6$, $\tau_0 = 0.6$, $\beta = 0.8$, $\lambda = \frac{1}{3}$ and $\theta = \tilde{\theta} = 0.7$ in `SOLVE` and `DATA`, respectively. The left plot in Figure 1 reports the $H^1(\Omega)$ -error versus the number of degrees of freedom ($\#\text{DoFs}$) when `GAL` is executed. We note that the error goes down almost vertically when we update the regularization radius after `INTERFACE`. In order to verify Theorem 4.16 (or Remark 4.17), we extract the sampling points only for U_j (i.e., the last Galerkin approximation in each iteration of `REGSOLVE`) and report the data in the right of (1). Based on the observation we confirm the first order rate of convergence. We also present our approximated solution U_3 and its underlying subdivision in (2).

We also test the algorithm in Remark 3.5 (i.e., we make one single iteration, and set the initial target tolerance to $\tau_0\beta^{j_{\max}}$), and report the energy error for the final approximation against $\#\text{DoFs}$ in Figure 3. Here we use the same parameters except that $j_{\max} = 14$, in order to reach a similar true error. Comparing with the right plot of Figure 1, we note that although both algorithms guarantee the quasi-optimal

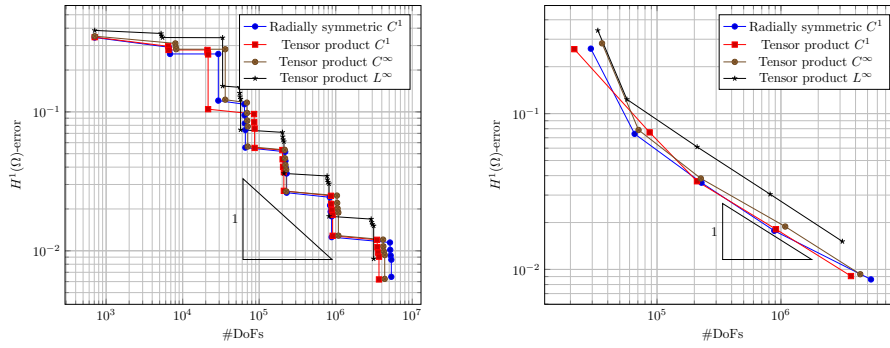


FIG. 1. Test on a L -shaped domain: (left) $H^1(\Omega)$ -error decay between the solution u and every Galerkin approximation (GAL) in REGSOLVE for different choices of $\delta^r(x)$. (right) $H^1(\Omega)$ -error decay between u and U_j defined in REGSOLVE. We set $j_{\max} = 6$, and $\tau_0 = .6$.

convergence rate, the energy error $\|U_{j_{\max}} - u\|$ using the algorithm in Remark 3.5 is much larger than that computed from REGSOLVE.

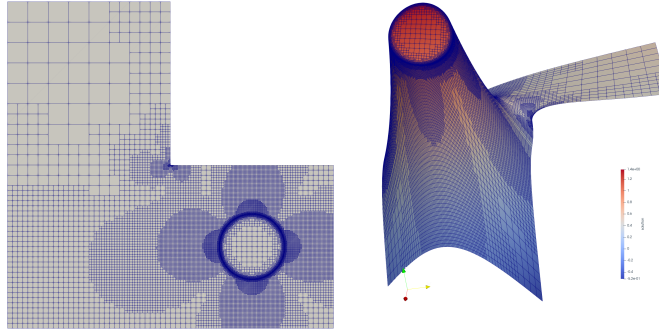


FIG. 2. Test on a L -shaped domain: (left) the subdivisions of U_3 in REGSOLVE and (right) the corresponding Galerkin approximation using Tensor product C^1 .

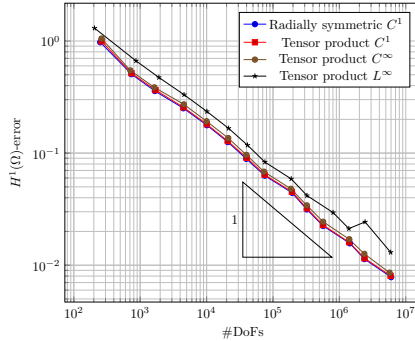


FIG. 3. Test on a L-shaped domain: $H^1(\Omega)$ -error decay between u and $U_{j_{\max}}$ defined from Remark 3.5. We set $j_{\max} = 6$, and $\tau_0 = .6$.

Now we consider (5.1) on the same L-shaped domain but using a L-shaped interface $\gamma = \partial\omega$ with $\omega = (-0.8, -0.2)^2 \setminus [-0.5, -0.2]^2$ and imposing zero Dirichlet boundary conditions on $\partial\Omega$. We set the same forcing data on γ , i.e., $f = 5$ and set $j_{\max} = 6$, $\tau_0 = 0.3$, $\beta = 0.6$, $\lambda = \frac{1}{3}$ and $\theta = \hat{\theta} = 0.8$. Since we do not have the analytic solution, we report the error indicator $\mathcal{E}(u^r, \mathcal{T})$ at each subdivision \mathcal{T} when GAL is executed. Figure 4 reports the error indicator $\mathcal{E}(u^r, \mathcal{T})$ against #DoFs. It shows that the error indicator decays in the rate 0.5, which is quasi-optimal. By Corollary 4.3, the subroutine INTERFACE guarantees the convergence rate 0.5 for the error from the regularization, the convergence rate of the total error should also be 0.5.

We have to point out that based on the vertical segments from the bottom left plot of Figure 4, the error indicator at $\tilde{\mathcal{T}}_j$, denoted by $\hat{\tau}_j$, is larger than that at \mathcal{T}_j , i.e., we cannot guarantee the decay of the error indicator along the whole process of REGSOLVE. According to (4.17), we guarantee that $\hat{\tau}_j \lesssim \tau_{j+1}$, which controls the jumps of such segments in Figure 4; see also Table 1 for all the ratios $\hat{\tau}_j/\tau_{j+1}$ for $j = 2, \dots, 7$. The approximated solution U_3 and the corresponding subdivision are also reported in Figure 5.

Tensor product C^1	1.754	1.365	1.150	1.293	1.127	1.227
Tensor product C^∞	1.976	1.487	1.246	1.375	1.215	1.293
Tensor product L^∞	1.969	1.442	1.348	1.449	1.212	1.349
Radially symmetric C^1	1.873	1.483	1.276	1.398	1.195	1.360

TABLE 1

Test in a L-shaped domain with an L-shaped interface: the ratio $\hat{\tau}_j/\tau_{j+1}$ for $j = 2, \dots, 7$ according to (4.17).

5.2. Convergence tests in the unit cube. We test our numerical algorithm in 3d by setting $\Omega = (-1, 1)^3$ and $\gamma = \partial B_R(c)$ with $R = 0.2$ and $c = (0.3, 0.3, 0.3)^T$. We also set the data function $f = \frac{1}{R^2}$ on γ and $g = 1/(|x - c|)$ so that the analytic

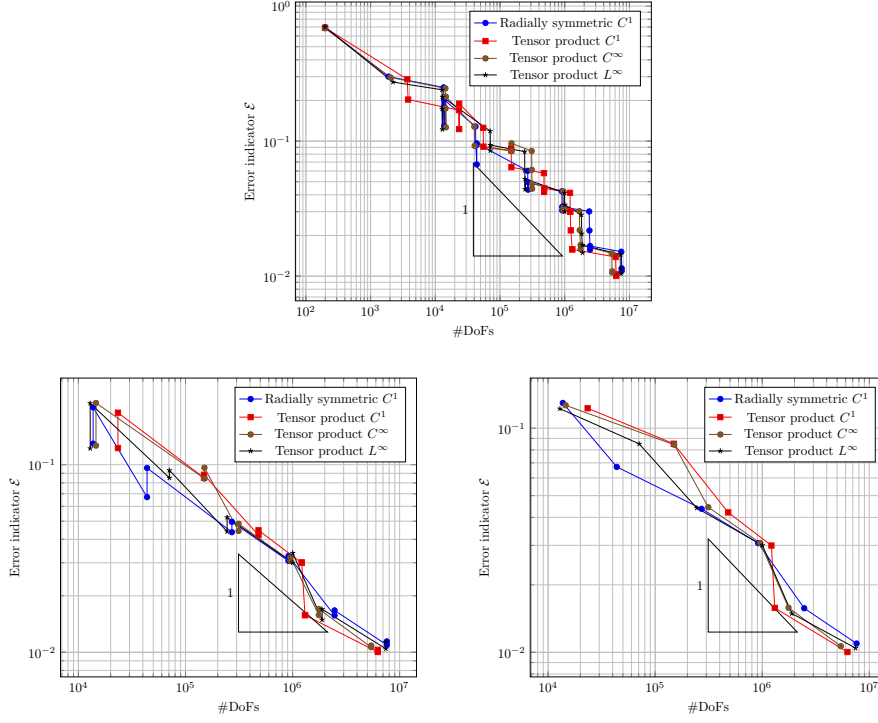


FIG. 4. Test on a L -shaped domain with an L -shaped interface: (top) decay of the error indicator for different choices of $\delta^v(x)$, (bottom left) error indicator plots for U_j and for the Galerkin approximations at \tilde{T}_j defined in REGSOLVE and (bottom right) error indicator plots only for U_j .

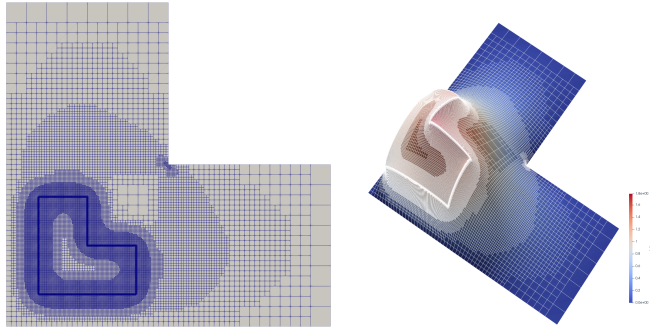


FIG. 5. Test on a L -shaped domain with an L -shaped interface: (left) the subdivisions of U_3 in REGSOLVE and (right) the corresponding Galerkin approximation using Tensor product C^1 .

solution is given by

$$u(x) = \begin{cases} \frac{1}{|x-c|}, & \text{if } |x-c| > R, \\ \frac{1}{R}, & \text{if } |x-c| \leq R. \end{cases}$$

We start with an initial uniform grid \mathcal{T}_0 with the mesh size $\sqrt{3}/16$. To approximate the interface γ , we start with initial quasi-uniform coarse mesh and refine it globally 7 times so that the geometric error is small enough. For the other approximation parameters, we set $j_{\max} = 5$, $\tau_0 = 1.5$, $\beta = 0.8$, $\lambda = 1$, $\theta = 0.5$ in SOLVE and $\tilde{\theta} = 0.8$ in DATA. In Figure 6, we report the $H^1(\Omega)$ -error against #DoFs for different types of δ^r . For each error plot, we also report the slope of the linear regression of the last five sampling points. For all choices of δ^r , the performance is not quasi-optimal. When using *radially symmetric* C^1 and *tensor product* C^1 , the convergence rates are better than the predicted one in Remark 4.17. We also report the coarse grid and the grids for U_5 and U_7 in Figure 7. The approximated solution U_7 using *radially symmetric* C^1 is provided in Figure 8.

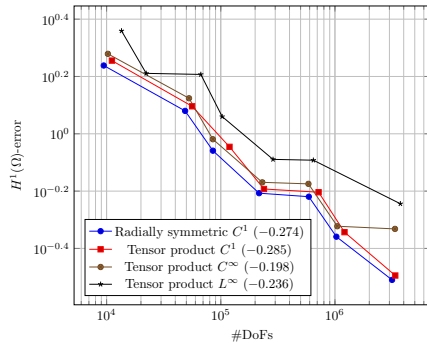


FIG. 6. Tests in the unit cube: $H^1(\Omega)$ -error decay between the solution u and U_j for $j = 1, \dots, 7$ and for different choices of $\delta^r(x)$. In terms of each plot, the slope of the linear regression of the last five sampling points is reported in the legend (these should be compared with the theoretical results which is -0.25 , and confirm our findings that the three-dimensional case is not quasi-optimal, which should result in a rate equal to -0.33).

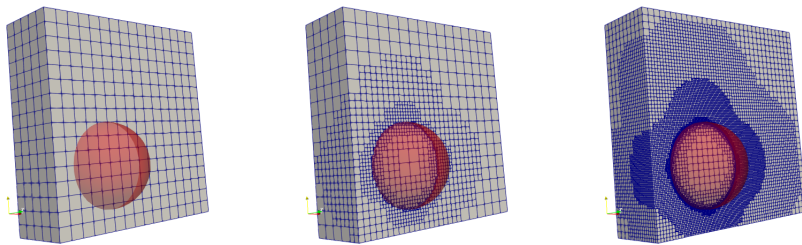


FIG. 7. Tests in the unit cube: the crinkle clip ($x_1 \leq 0.3$) of the coarse grid (left) as well as the subdivisions for U_5 (mid) and U_7 (right) using *radially symmetric* C^1 . The interface γ is marked in red.

5.3. Performance tests in the unit square. Consider $\Omega = (0, 1)^2$, $\gamma = \partial B_R(c)$ with $R = 0.2$ and $c = (0.3, 0.3)^{\text{tr}}$, $f = \frac{1}{R}$ and $g = \ln(|x - c|)$. Similar to

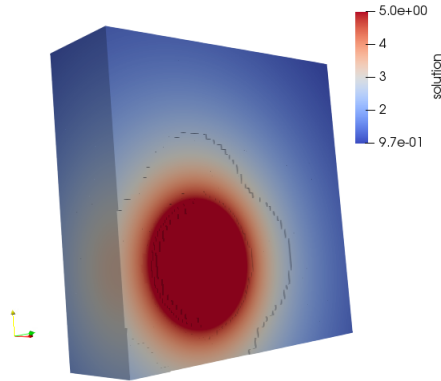


FIG. 8. Tests in the unit cube: the crinkle clip ($x_1 \leq 0.3$) of the approximation U_7 using radially symmetric C^1 (3741904 DoFs).

the previous section, we can obtain the following exact solution

$$u(x) = \begin{cases} -\ln(|x - c|), & \text{if } |x - c| > R, \\ -\ln(R), & \text{if } |x - c| \leq R. \end{cases}$$

We shall compare the performance of our numerical algorithms both in Algorithm 3.9 and Remark 3.5 with the algorithm without regularization; see the numerical algorithm from Section 7.2 of [15]. To be more precise, the algorithm without using the regularization is based on SOLVE by replacing the data indicator \mathcal{D} with the following surrogate data indicator:

$$\tilde{D}(f, T, \mathcal{T}) := h_T^{1/2} \|f\|_{L^2(T \cap \gamma)}.$$

Using the exact solution u , after the j -th iterate of REGSOLVE in Algorithm 3.9 using tensor product L^∞ , we compute the $H^1(\Omega)$ -error between u and U_j , denoted by e_j . For the parameters we set $\tau_0 = 0.3$, $\beta = 0.7$, $\lambda = \frac{1}{3}$, $\theta = \tilde{\theta} = 0.55$. Then we run the non-regularized program with the same parameters and terminate it when the energy error is smaller than e_j , denoting \tilde{e}_j the energy error for the corresponding output approximation. For $j = 8, 9, \dots, 12$. We also compute e_j using the algorithm provided by Remark 3.5 with $j = 11, \dots, 15$. Now we report those errors and the CPU times for each program against #DoFs in Figure 10. We observe that all algorithms are quasi-optimal but the algorithm from Remark 3.5 requires more DoFs. In terms of the computations time, it turns out that Algorithm 3.9 needs more time when the discrete system is small (less than 10^7) and become more efficient when the size of the system is increasing. In Figure 11, we finally report the grid for U_5 using Algorithm 3.9 and corresponding grid for the non-regularized algorithm.

6. Conclusion and outlook. We have proposed an adaptive finite element algorithm to approximate the solutions of elliptic problems with rough data approximated by regularization. Such problems are relevant in many applications ranging from fluid-structure interaction, to the modeling of biomedical applications with complex embedded domains or networks.

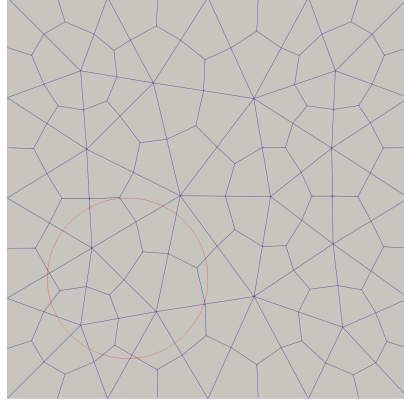


FIG. 9. Tests on a square: the unstructured coarse mesh T_0 . The interface γ is marked in red.

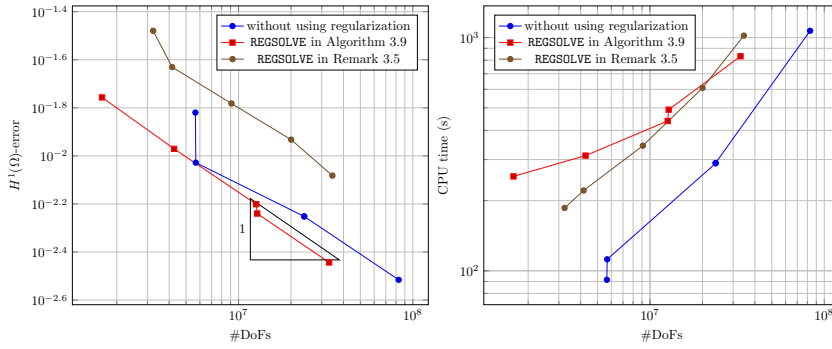


FIG. 10. Tests on a square: (left) $\|U_j - u\|_{H^1(\Omega)}$ using REGSOLVE with tensor product L^∞ for $j = 8, \dots$ and the corresponding $H^1(\Omega)$ -error decay without using the regularization; (right) computational time against $\#nDoFs$ for two adaptive algorithms. We note that the sampling points for the non-regularized algorithm at $j = 10$ and 11 are so closed that they overlap with each other.

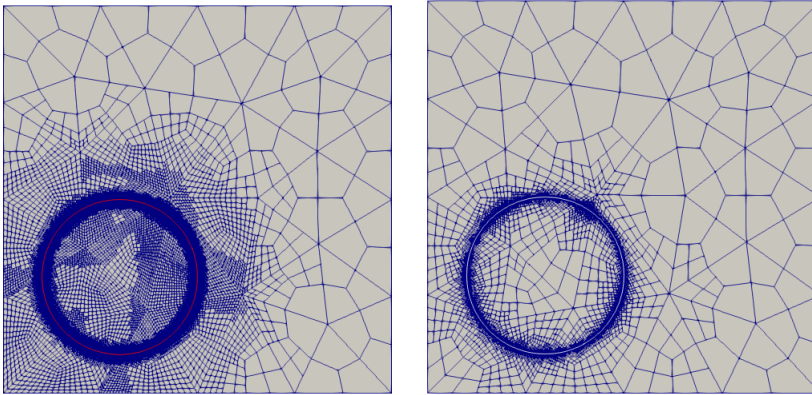


FIG. 11. Tests on a square: (left) the subdivision for U_5 and (right) the corresponding subdivision using non-regularized algorithm.

Our approach builds on classical results for adaptive finite element theory for H^{-1} data, and for L^2 data. What characterizes the regularization process is that, even if the resulting forcing term is as regular as desired – at fixed regularization parameter r – its regularity does not hold uniformly with respect to r .

This observation suggests that one could exploit the knowledge of the asymptotic behavior of the data regularity with respect to r to construct an algorithm that a-priorily refines around the rough part of the forcing term, in a way that guarantees quasi optimal convergence, at least in the two dimensional case.

The resulting approximation error is split into a regularization error for u and the finite element approximation error for the regularized u^r . In this work we show how to control the dependencies between these two errors and provide an algorithm in which the error decay in the energy norm is quasi-optimal in two dimensional space and sub-optimal in three dimensional space.

Our findings are specific for the co-dimension one case, but could be easily extended to the co-dimension zero case, where the dependency of the regularity on r disappears naturally, due to the intrinsic L^2 nature of the resulting forcing term.

Appendix A. Contraction property of SOLVE. This section is devoted to reviewing the contraction property of the SOLVE module. Let us first recall from [15, Lemma 4.1] the reduction property of the jump residual. Given a conforming refinement \mathcal{T} of \mathcal{T}_0 and a subset \mathcal{M} of \mathcal{T} , set \mathcal{T}^* be any conforming refinement of $\text{REFINE}(\mathcal{T}, \mathcal{M})$. Letting $V \in \mathbb{V}(\mathcal{T})$ and $V^* \in \mathbb{V}(\mathcal{T}^*)$, there exists a positive constant C_{JR} so that for all $\delta > 0$,

$$(A.1) \quad \begin{aligned} \mathcal{J}(V^*, \mathcal{T}^*)^2 &\leq (1 + \delta) \left(\mathcal{J}(V, \mathcal{T})^2 - \frac{1}{2} \mathcal{J}(V, \mathcal{M})^2 \right) \\ &\quad + (1 + \delta^{-1}) C_{\text{JR}} \|V^* - V\|_{H_0^1(\Omega)}^2. \end{aligned}$$

In terms of the reduction of the data indicator, we note that from the subdivision \mathcal{T} to its refinement \mathcal{T}^* , if a cell $T \in \mathcal{T}$ is bisected b times, we have $|T^*| = 2^{-b}|T|$ for each cell $T^* \subset T$. This implies that $h_{T^*} = 2^{-b/d}h_T$ and for $g \in L^2(\Omega)$,

$$\sum_{T^* \in \mathcal{T}^*, T^* \subset T} h_{T^*}^2 \|g\|_{L^2(T^*)}^2 = 2^{-2b/d} h_T^2 \|g\|_{L^2(T)}^2.$$

Thus, we conclude that

$$(A.2) \quad \mathcal{D}(g, \mathcal{T}^*) \leq \mathcal{D}(g, \mathcal{T}).$$

Moreover, if a refinement subset \mathcal{M} of \mathcal{T} is defined as in DATA and \mathcal{T}^* is the output of $\text{REFINE}(\mathcal{T}, \mathcal{M})$, there holds the contraction property of DATA,

$$(A.3) \quad \begin{aligned} \mathcal{D}(g, \mathcal{T}^*)^2 &\leq \mathcal{D}(g, \mathcal{T}^* \setminus \mathcal{M})^2 + 2^{-1/d} \mathcal{D}(g, \mathcal{M})^2 \\ &= \mathcal{D}(g, \mathcal{T})^2 - (1 - 2^{-1/d}) \mathcal{D}(g, \mathcal{M})^2 \\ &\leq \mathcal{D}(g, \mathcal{T})^2 - (1 - 2^{-1/d}) \tilde{\theta} \mathcal{D}(g, \mathcal{T})^2 \\ &= \eta^2 \mathcal{D}(g, \mathcal{T})^2 \end{aligned}$$

with $\eta^2 = 1 - (1 - 2^{-1/d}) \tilde{\theta} \leq 1$.

LEMMA A.1 (error reduction). *Given a bulk parameter $\theta \in (0, 1)$, we assume that $\lambda < \min(1, \sqrt{2/(5\theta)})$ in SOLVE. Let $\{W_k, \mathcal{T}_k\}$ be defined as in SOLVE. Then there*

holds that for $\delta > 0$,

$$\begin{aligned} \mathcal{E}(W_{k+1}, \mathcal{T}_{k+1})^2 &\leq (1 + \delta) \left(1 - \frac{3}{4} \lambda^2 \theta^2 \right) \mathcal{E}(W_k, \mathcal{T}_k)^2 + (1 + \delta^{-1}) C_{\text{JR}} \|W_{k+1} - W_k\|_{H_0^1(\Omega)}^2. \end{aligned}$$

Proof. Denote $\mathcal{E}_k := \mathcal{E}(W_k, \mathcal{T}_k)$, $\mathcal{J}_k := \mathcal{J}(W_k, \mathcal{T}_k)$ and $\mathcal{D}_k := \mathcal{D}(g, \mathcal{T}_k)$. We shall bound the target estimate based on the criteria $\mathcal{D}_k \leq \lambda \theta \mathcal{E}_k$. If it is true, we invoke the bulk property (3.5) to get

$$\begin{aligned} \theta^2 \mathcal{E}_k^2 &\leq \mathcal{E}(W_k, \mathcal{M}_k)^2 \\ &= \mathcal{J}(W_k, \mathcal{M}_k)^2 + \mathcal{D}_k^2 \leq \mathcal{J}(W_k, \mathcal{M}_k)^2 + \lambda^2 \theta^2 \mathcal{E}_k^2 \end{aligned}$$

This and the assumption of λ show that

$$\mathcal{J}(W_k, \mathcal{M}_k)^2 \geq (1 - \lambda^2) \mathcal{D}_k^2.$$

using the above estimate together with the reduction properties (A.1) and (A.2) to obtain that

$$\begin{aligned} \mathcal{E}_{k+1}^2 &= \mathcal{J}_{k+1}^2 + \mathcal{D}_{k+1}^2 \\ &\leq (1 + \delta) \left(\mathcal{J}_k^2 - \frac{1}{2} \mathcal{J}(W_k, \mathcal{M}_k)^2 \right) + (1 + \delta^{-1}) C_{\text{JR}} \|W_{k+1} - W_k\|_{H_0^1(\Omega)}^2 + \mathcal{D}_{k+1}^2 \\ &\leq (1 + \delta) \left(\mathcal{J}_k^2 - \frac{1}{2} \mathcal{J}(W_k, \mathcal{M}_k)^2 + \mathcal{D}_k^2 \right) + (1 + \delta^{-1}) C_{\text{JR}} \|W_{k+1} - W_k\|_{H_0^1(\Omega)}^2 \\ &\leq \frac{1}{2} (1 + \delta) (1 + \lambda^2) \mathcal{E}_k^2 + (1 + \delta^{-1}) C_{\text{JR}} \|W_{k+1} - W_k\|_{H_0^1(\Omega)}^2. \end{aligned}$$

This together with the assumption of λ implies the target estimate.

If $\mathcal{D}_k \geq \lambda \theta \mathcal{E}_k$, DATA is called the loop of SOLVE. The contraction property (A.3) guarantees that DATA terminates satisfying

$$\mathcal{D}_{k+1}^2 \leq \frac{\sigma_k^2}{4} = \frac{\lambda^2 \theta^2}{4} \mathcal{E}_k.$$

By the definition of \mathcal{E}_k we also have $\mathcal{J}_k^2 < (1 - \lambda^2 \theta^2) \mathcal{E}_k^2$. Combing the above two estimates into (A.1) yields

$$\begin{aligned} \mathcal{E}_{k+1}^2 &\leq (1 + \delta) (\mathcal{J}_k^2 + \mathcal{D}_{k+1}^2) + (1 + \delta^{-1}) C_{\text{JR}} \|W_{k+1} - W_k\|_{H_0^1(\Omega)}^2 \\ &\leq (1 + \delta) \left(1 - \frac{3}{4} \lambda^2 \theta^2 \right) \mathcal{E}_k^2 + (1 + \delta^{-1}) C_{\text{JR}} \|W_{k+1} - W_k\|_{H_0^1(\Omega)}^2. \end{aligned}$$

Again we obtain the desired estimate and the proof is complete. \square

We are now in a position to show Theorem 4.4.

Proof of Theorem 4.4. We invoke Lemma A.1 and the following Galerkin orthogonality

$$\|w_g - W_{k+1}\|^2 = \|w_g - W_k\|^2 - \|W_{k+1} - W_k\|^2$$

to derive that

$$\begin{aligned} \|w_g - W_{k+1}\|^2 &+ \tilde{\alpha} \mathcal{E}_{k+1}^2 \\ &\leq \|w_g - W_k\|^2 + (\tilde{\alpha} (1 + \delta^{-1}) C_{\text{JR}} - 1) \|W_{k+1} - W_k\|^2 \\ &\quad + \tilde{\alpha} (1 + \delta) \left(1 - \frac{3}{4} \lambda^2 \theta^2 \right) \mathcal{E}_k^2. \end{aligned}$$

We shall determine the values of δ and $\tilde{\alpha}$ so that the right hand side above is bounded by target estimate. We first apply the global upper bound (3.8) to yield

$$\left(1 - \frac{3}{4}\lambda^2\theta^2\right)\mathcal{E}_k^2 \leq \left(1 - \frac{3}{8}\lambda^2\theta^2\right)\mathcal{E}_k^2 - \frac{3}{8C_{\text{rel}}^2}\lambda^2\theta^2\|w_g - W_k\|^2.$$

This leads to

$$\begin{aligned} \|w_g - W_{k+1}\|^2 + \tilde{\alpha}\mathcal{E}_{k+1}^2 &\leq \left(1 - \tilde{\alpha}(1 + \delta)\frac{3}{8C_{\text{rel}}^2}\lambda^2\theta^2\right)\|w_g - W_k\|^2 \\ &\quad + (\tilde{\alpha}(1 + \delta^{-1})C_{\text{JR}} - 1)\|W_{k+1} - W_k\|^2 \\ &\quad + \tilde{\alpha}(1 + \delta)\left(1 - \frac{3}{8}\lambda^2\theta^2\right)\mathcal{E}_k^2. \end{aligned}$$

Now we choose δ so that

$$(1 + \delta)\left(1 - \frac{3}{8}\lambda^2\theta^2\right) = 1 - \frac{3}{16}\lambda^2\theta^2.$$

Based on the above choice we set $\tilde{\alpha}$ so that

$$\tilde{\alpha}(1 + \delta^{-1})C_{\text{JR}} - 1 = 0.$$

Therefore, we arrive at

$$\begin{aligned} \|w_g - W_{k+1}\|^2 + \tilde{\alpha}\mathcal{E}_{k+1}^2 &\leq \left(1 - \frac{3\delta}{8C_{\text{rel}}^2C_{\text{JR}}}\lambda^2\theta^2\right)\|w_g - W_k\|^2 + \tilde{\alpha}\left(1 - \frac{3}{16}\lambda^2\theta^2\right)\mathcal{E}_k^2. \end{aligned}$$

The proof is complete by choosing

$$\alpha^2 := \max\left(1 - \frac{3\delta}{8C_{\text{rel}}^2C_{\text{JR}}}\lambda^2\theta^2, 1 - \frac{3}{16}\lambda^2\theta^2\right) < 1. \quad \square$$

Proof of Corollary 4.9. We first show that the data indicator satisfies the following bulk property: recalling that $\tilde{\theta}$ is the bulk parameter, let $\mu = (1 - \tilde{\theta}^2)^{1/2}$ and \mathcal{T}^+ be a refinement of \mathcal{T} satisfying $\mathcal{D}(F^r, \mathcal{T}^+) \leq \mu\mathcal{D}(F^r, \mathcal{T})$. Then, $\mathcal{D}(F^r, \mathcal{R}_{\mathcal{T} \rightarrow \mathcal{T}^+}) \geq \tilde{\theta}\mathcal{D}(F^r, \mathcal{T})$. In fact,

$$\begin{aligned} \mathcal{D}(F^r, \mathcal{T}^+ \setminus \mathcal{R}_{\mathcal{T} \rightarrow \mathcal{T}^+})^2 + \mathcal{D}(F^r, \mathcal{R}_{\mathcal{T} \rightarrow \mathcal{T}^+})^2 &= \mathcal{D}(F^r, \mathcal{T}^+)^2 \\ &\leq \mu^2\mathcal{D}(F^r, \mathcal{T}) = \mu^2\mathcal{D}(F^r, \mathcal{T} \setminus \mathcal{R}_{\mathcal{T} \rightarrow \mathcal{T}^+})^2 + \mu^2\mathcal{D}(F^r, \mathcal{R}_{\mathcal{T} \rightarrow \mathcal{T}^+})^2 \end{aligned}$$

Noting that $\mathcal{D}(F^r, \mathcal{T}^+ \setminus \mathcal{R}_{\mathcal{T} \rightarrow \mathcal{T}^+}) = \mathcal{D}(F^r, \mathcal{T} \setminus \mathcal{R}_{\mathcal{T} \rightarrow \mathcal{T}^+})$, we obtain that

$$(1 - \mu^2)\mathcal{D}(F^r, \mathcal{T}) \leq \mu^2\mathcal{D}(F^r, \mathcal{R}_{\mathcal{T} \rightarrow \mathcal{T}^+}).$$

Applying $\mu = (1 - \tilde{\theta}^2)^{1/2}$ implies the bulk property.

Suppose that there are totally J iterations executed in DATA. For $j = 1, \dots, J$, denote \mathcal{T}^j the resulting subdivision at each iteration and \mathcal{R}^j the collection of cells generated by MARK. By convention, we set $\mathcal{T}^0 = \mathcal{T}$ and denote $\mathcal{D}^j := \mathcal{D}(F^r, \mathcal{T}^j)$. For

each j , according to Lemma 4.7, there exists a conforming refinement $\mathcal{T}^{\mu,j}$ of $\tilde{\mathcal{T}}$ such that $\mathcal{T}^{\mu,j} \leq \mu \mathcal{D}^j$ and

$$\#(\mathcal{T}^{\mu,j}) - \#(\tilde{\mathcal{T}}) \lesssim r^{1-d/2}(\mu \mathcal{D}^j)^{-d}.$$

So the overlay $\tilde{\mathcal{T}}^{\mu,j} := \mathcal{T}^j \oplus \mathcal{T}^{\mu,j}$ satisfies $\mathcal{D}(F^r, \tilde{\mathcal{T}}^{\mu,j}) \leq \mu \mathcal{D}^j$, which, according to the bulk property, implies that

$$\#(\mathcal{R}^j) \leq \#(\mathcal{R}_{\mathcal{T}^j \rightarrow \tilde{\mathcal{T}}^{\mu,j}}) \lesssim \#(\tilde{\mathcal{T}}^{\mu,j}) - \#(\mathcal{T}^j) \leq \#(\mathcal{T}^{\mu,j}) - \#(\tilde{\mathcal{T}}) \lesssim r^{1-d/2}(\mu \mathcal{D}^j)^{-d}.$$

Using the contraction property (A.3) (i.e., $\mathcal{D}^j \leq \eta \mathcal{D}^{j-1}$) and $\mathcal{D}^{J-1} \geq \tau$, the total refined cells in DATA can be controlled by

$$\sum_{j=0}^{J-1} \#(\mathcal{R}^j) \lesssim r^{1-d/2} \sum_{j=0}^{J-1} (\mathcal{D}^j)^{-jd} \lesssim r^{1-d/2} \tau^{-d} \sum_{j=0}^{J-1} \eta^{dj} \lesssim r^{1-d/2} \tau^{-d}.$$

The proof is complete. \square

REFERENCES

- [1] A. ALLENDES, E. OTÁROLA, AND A. J. SALGADO, *A posteriori error estimates for the stokes problem with singular sources*, Computer Methods in Applied Mechanics and Engineering, 345 (2019), pp. 1007–1032, <https://doi.org/10.1016/j.cma.2018.11.004>.
- [2] G. ALZETTA AND L. HELTAI, *Multiscale modeling of fiber reinforced materials via non-matching immersed methods*, Computers & Structures, 239 (2020), p. 106334, <https://doi.org/10.1016/j.compstruc.2020.106334>.
- [3] D. ARNDT, W. BANGERTH, B. BLAIS, T. C. CLEVINGER, M. FEHLING, A. V. GRAYVER, T. HEISTER, L. HELTAI, M. KRONBICHLER, M. MAIER, P. MUNCH, J.-P. PELTERET, R. RASTAK, I. THOMAS, B. TURCK SIN, Z. WANG, AND D. WELLS, *The deal.II library, version 9.2*, J. Numer. Math., 28 (2020), pp. 131–146, <https://doi.org/10.1515/jnma-2020-0043>.
- [4] R. E. BANK AND A. WEISER, *Some a posteriori error estimators for elliptic partial differential equations*, Math. Comp., 44 (1985), pp. 283–301, <https://doi.org/10.2307/2007953>.
- [5] S. BERTOLUZZA, A. DECOENE, L. LACOUTURE, AND S. MARTIN, *Local error estimates of the finite element method for an elliptic problem with a dirac source term*, Numerical Methods for Partial Differential Equations, 34 (2017), pp. 97–120, <https://doi.org/10.1002/num.22186>.
- [6] P. BINEV, W. DAHMEN, AND R. DEVORE, *Adaptive finite element methods with convergence rates*, Numer. Math., 97 (2004), pp. 219–268, <https://doi.org/10.1007/s00211-003-0492-7>.
- [7] P. BINEV, W. DAHMEN, R. DEVORE, AND P. PETRUSHEV, *Approximation classes for adaptive methods*, Serdica Math. J., 28 (2002), pp. 391–416. Dedicated to the memory of Vassil Popov on the occasion of his 60th birthday.
- [8] D. BOFFI AND L. GASTALDI, *A finite element approach for the immersed boundary method*, Comput. & Structures, 81 (2003), pp. 491–501, [https://doi.org/10.1016/S0045-7949\(02\)00404-2](https://doi.org/10.1016/S0045-7949(02)00404-2). In honour of Klaus-Jürgen Bathe.
- [9] D. BOFFI AND L. GASTALDI, *On the existence and the uniqueness of the solution to a fluid-structure interaction problem*, Journal of Differential Equations, 279 (2021), pp. 136–161, <https://doi.org/10.1016/j.jde.2021.01.019>.
- [10] A. BONITO, R. A. DEVORE, AND R. H. NOCHETTO, *Adaptive finite element methods for elliptic problems with discontinuous coefficients*, SIAM J. Numer. Anal., 51 (2013), pp. 3106–3134, <https://doi.org/10.1137/130905757>.
- [11] A. BONITO AND R. H. NOCHETTO, *Quasi-optimal convergence rate of an adaptive discontinuous Galerkin method*, SIAM J. Numer. Anal., 48 (2010), pp. 734–771, <https://doi.org/10.1137/08072838X>.
- [12] J. M. CASCON, C. KREUZER, R. H. NOCHETTO, AND K. G. SIEBERT, *Quasi-optimal convergence rate for an adaptive finite element method*, SIAM J. Numer. Anal., 46 (2008), pp. 2524–2550, <https://doi.org/10.1137/07069047X>.

- [13] D. CERRONI, F. LAURINO, AND P. ZUNINO, *Mathematical analysis, finite element approximation and numerical solvers for the interaction of 3d reservoirs with 1d wells*, GEM - International Journal on Geomathematics, 10 (2019), <https://doi.org/10.1007/s13137-019-0115-9>.
- [14] P. G. CIARLET, *The finite element method for elliptic problems*, vol. 40 of Classics in Applied Mathematics, Society for Industrial and Applied Mathematics (SIAM), Philadelphia, PA, 2002, <https://doi.org/10.1137/1.9780898719208>. Reprint of the 1978 original [North-Holland, Amsterdam; MR0520174 (58 #25001)].
- [15] A. COHEN, R. DEVORE, AND R. H. NOCHETTO, *Convergence rates of AFEM with H^{-1} data*, Found. Comput. Math., 12 (2012), pp. 671–718, <https://doi.org/10.1007/s10208-012-9120-1>.
- [16] A. DEMLOW, *Higher-order finite element methods and pointwise error estimates for elliptic problems on surfaces*, SIAM J. Numer. Anal., 47 (2009), pp. 805–827, <https://doi.org/10.1137/070708135>.
- [17] A. DEMLOW AND G. DZIUK, *An adaptive finite element method for the Laplace-Beltrami operator on implicitly defined surfaces*, SIAM J. Numer. Anal., 45 (2007), pp. 421–442, <https://doi.org/10.1137/050642873>.
- [18] W. DÖRFLER, *A convergent adaptive algorithm for Poisson's equation*, SIAM J. Numer. Anal., 33 (1996), pp. 1106–1124, <https://doi.org/10.1137/0733054>.
- [19] W. DÖRFLER AND R. H. NOCHETTO, *Small data oscillation implies the saturation assumption*, Numer. Math., 91 (2002), pp. 1–12, <https://doi.org/10.1007/s002110100321>.
- [20] A. ERN AND J.-L. GUERMOND, *Theory and practice of finite elements*, vol. 159 of Applied Mathematical Sciences, Springer-Verlag, New York, 2004, <https://doi.org/10.1007/978-1-4757-4355-5>.
- [21] D. GILBARG AND N. S. TRUDINGER, *Elliptic partial differential equations of second order*, Classics in Mathematics, Springer-Verlag, Berlin, 2001. Reprint of the 1998 edition.
- [22] P. GRISVARD, *Elliptic problems in nonsmooth domains*, vol. 24 of Monographs and Studies in Mathematics, Pitman (Advanced Publishing Program), Boston, MA, 1985.
- [23] L. HELTAI AND A. CAIAZZO, *Multiscale modeling of vascularized tissues via nonmatching immersed methods*, Int. J. Numer. Methods Biomed. Eng., 35 (2019), pp. e3264, 32, <https://doi.org/10.1002/cnm.3264>.
- [24] L. HELTAI, A. CAIAZZO, AND L. O. MÜLLER, *Multiscale coupling of one-dimensional vascular models and elastic tissues*, Annals of Biomedical Engineering, (2021).
- [25] L. HELTAI AND F. COSTANZO, *Variational implementation of immersed finite element methods*, Comput. Methods Appl. Mech. Engrg., 229/232 (2012), pp. 110–127, <https://doi.org/10.1016/j.cma.2012.04.001>.
- [26] L. HELTAI AND W. LEI, *A priori error estimates of regularized elliptic problems*, Numer. Math., 146 (2020), pp. 571–596, <https://doi.org/10.1007/s00211-020-01152-w>.
- [27] L. HELTAI AND N. ROTUNDO, *Error estimates in weighted sobolev norms for finite element immersed interface methods*, Computers & Mathematics with Applications, 78 (2019), pp. 3586–3604.
- [28] B. HOSSEINI, N. NIGAM, AND J. M. STOCKIE, *On regularizations of the Dirac delta distribution*, J. Comput. Phys., 305 (2016), pp. 423–447, <https://doi.org/10.1016/j.jcp.2015.10.054>.
- [29] P. HOUSTON AND T. P. WIHLER, *Discontinuous galerkin methods for problems with dirac delta source*, Mathematical Modelling and Numerical Analysis, 46 (2012), pp. 1467–1483, <https://doi.org/10.1051/m2an/2012010>.
- [30] H. LI, X. WAN, P. YIN, AND L. ZHAO, *Regularity and finite element approximation for two-dimensional elliptic equations with line dirac sources*, Journal of Computational and Applied Mathematics, 393 (2021), p. 113518, <https://doi.org/10.1016/j.cam.2021.113518>.
- [31] F. MILLAR, I. MUGA, S. ROJAS, AND K. G. V. DER ZEE, *Projection in negative norms and the regularization of rough linear functionals*, 2021, <https://arxiv.org/abs/2101.03044>.
- [32] W. F. MITCHELL, *A comparison of adaptive refinement techniques for elliptic problems*, ACM Trans. Math. Software, 15 (1989), pp. 326–347 (1990), <https://doi.org/10.1145/76909.76912>.
- [33] R. MITTAL AND G. IACCARINO, *Immersed boundary methods*, in Annual review of fluid mechanics. Vol. 37, vol. 37 of Annu. Rev. Fluid Mech., Annual Reviews, Palo Alto, CA, 2005, pp. 239–261, <https://doi.org/10.1146/annurev.fluid.37.061903.175743>.
- [34] R. H. NOCHETTO, K. G. SIEBERT, AND A. VEESER, *Theory of adaptive finite element methods: an introduction*, in Multiscale, nonlinear and adaptive approximation, Springer, Berlin, 2009, pp. 409–542, https://doi.org/10.1007/978-3-642-03413-8_12.
- [35] C. S. PESKIN, *The immersed boundary method*, Acta Numer., 11 (2002), pp. 479–517, <https://doi.org/10.1017/S0962492902000077>.

- [36] D. D. SILVA, F. FERRARI, AND S. SALSA, *Perron's solutions for two-phase free boundary problems with distributed sources*, *Nonlinear Analysis: Theory, Methods & Applications*, 121 (2015), pp. 382–402, <https://doi.org/10.1016/j.na.2015.02.013>.
- [37] R. STEVENSON, *An optimal adaptive finite element method*, *SIAM J. Numer. Anal.*, 42 (2005), pp. 2188–2217, <https://doi.org/10.1137/S0036142903425082>.
- [38] R. STEVENSON, *Optimality of a standard adaptive finite element method*, *Found. Comput. Math.*, 7 (2007), pp. 245–269, <https://doi.org/10.1007/s10208-005-0183-0>.
- [39] R. STEVENSON, *The completion of locally refined simplicial partitions created by bisection*, *Math. Comp.*, 77 (2008), pp. 227–241, <https://doi.org/10.1090/S0025-5718-07-01959-X>.
- [40] J.-P. SUAREZ, G. B. JACOBS, AND W.-S. DON, *A high-order dirac-delta regularization with optimal scaling in the spectral solution of one-dimensional singular hyperbolic conservation laws*, *SIAM Journal on Scientific Computing*, 36 (2014), pp. A1831–A1849, <https://doi.org/10.1137/130939341>.
- [41] A.-K. TORNBORG, *Multi-dimensional quadrature of singular and discontinuous functions*, *BIT*, 42 (2002), pp. 644–669, <https://doi.org/10.1023/A:1021988001059>.